

Sparse learning of chemical reaction networks from trajectory data

Wei Zhang¹, Stefan Klus², Tim Conrad², and Christof Schütte^{1,2}

Abstract

In this paper, we develop a data-driven numerical method to learn chemical reaction networks from trajectory data. Modeling the reaction system as a continuous-time Markov chain, our method learns the propensity functions of the system with predetermined basis functions by maximizing the likelihood function of the trajectory data under l^1 sparse regularization. We demonstrate our method with numerical examples, and we perform asymptotic analysis of the proposed learning procedure in the infinite-data limit.

Keywords chemical reactions, inverse problems, data-driven methods, l^1 sparse optimization, asymptotic analysis

1 Introduction

Chemical reaction networks [19, 1] have been shown to be very useful in studying dynamical processes in chemistry and biology, where systems under investigation typically contain many different reactants that interact with each other. In in-silico biology, for instance, the cellular processes are often modeled as cellular reaction networks (CRNs), which take the relevant biological/chemical components as well as their interactions into account [20, 6, 35, 29]. Modeling cellular processes, or finding the kinetic structures of the underlying cellular reaction networks [43, 11, 13, 33, 41, 26], is one of the most prominent fields of in-silico biology due to the important role of such models in understanding the cellular behavior. This task is particularly challenging for realistic CRNs that are characterized by a large number of elements and interactions (reactions). At the same time, more and more trajectory data of cellular processes are becoming available, thanks to the state-of-the-art single-cell based laboratory techniques.

The aim of the current work is to develop data-driven methods [27] that allow to learn chemical reaction networks from trajectory data and to apply the new methods to the modeling of cellular processes. Given the trajectory data of a stochastic chemical reaction process, we propose a numerical approach to reconstruct the underlying reaction network by maximizing the likelihood function of the trajectory with sparsity regularization. Roughly speaking, our approach consists of three steps. In the first step, preliminary information of the reaction network, such as the number of different elements (reactant, products) and the total number of reaction channels, is extracted from trajectory data by counting and enumerating. Based on this information, in the second step, we prepare several basis functions which will be used

¹Zuse Institute Berlin, D-14195 Berlin, Germany

²Institut für Mathematik, Freie Universität Berlin, D-14195 Berlin, Germany

in learning the propensity functions of the reaction network. The theory of chemical reactions suggests that we can choose each basis function as the product of copy-numbers of at most two different reactants [2, 14]. In the third step, the propensity function of each reaction channel is represented using linear combinations of the basis functions involving unknown coefficients, which are then determined by maximizing the log-likelihood function of the trajectory data together with sparse regularization using l^1 -norm [22].

In contrast to Lasso [38, 39], the optimization problem that needs to be solved in our learning approach is a nonlinear sparse optimization problem, due to the nonlinearity of the log-likelihood function of the reaction network. In our study, we find that the FISTA (Fast Iterative Shrinkage-Thresholding Algorithm) proposed in [7] is a suitable algorithm for solving our problem. We also propose a simple preconditioning technique which will significantly improve the performance of the numerical algorithm by allowing larger step-sizes in FISTA. This preconditioning technique turns out to be particularly useful when the basis functions take values at different orders of magnitudes for the given trajectory data. On the theoretical side, in this paper we also provide an asymptotic analysis of our learning approach in the infinite-data limit. Under certain technical assumptions, by applying the large sample theory [16, 28], we establish the asymptotic consistency and the asymptotic normality of the estimators in our learning procedure, which therefore provides a solid theoretical ground for the data-driven method proposed in this paper.

Before concluding the introduction, let us review related work and also summarize the contribution of this paper. The reconstruction of the governing equations of dynamical systems using sparsity has been studied recently in [42, 10, 31, 13] for ordinary differential equations (ODEs) and in [8] for stochastic differential equations (SDEs). For chemical and biological reaction systems, the problem of estimating unknown parameters has been well studied when the systems are modeled both as ODEs [23, 3] and as continuous-time Markov chain processes [1, 34, 9, 43], while the reconstruction of the entire chemical reaction networks, i.e., finding parsimonious models, has only been considered when the systems are modeled as ODE systems [41, 31, 13]. We refer to the nice review [41] for recent developments on the reverse engineering in system biology. Compared to the aforementioned existing results, our work is new in the following three aspects. Firstly, we study sparse reconstruction of chemical reaction networks as continuous-time Markov chains, which, to the best of our knowledge, has not been considered in the literature. Comparing to ODE models, continuous-time Markov chain as a stochastic model provides more details of reaction systems due to its ability to capture stochastic effects, which can play an important role for cellular processes [37, 36, 25]. Secondly, we develop numerical codes in which we implement the FISTA method [7] to solve a nonlinear sparse optimization problem in order to learn the reaction networks from trajectory data. Our numerical experience, in particular the preconditioning technique, may be useful in other sparse optimization problems as well. Thirdly, we provide theoretical basis of the data-driven method proposed in the current paper. Notice that, although different data-driven methods using sparsity [42, 10, 8] have been developed in the literature for different types of dynamical systems, the theoretical analysis of these methods is far away from being complete (see [40]). We expect the theoretical analysis presented in our work can shed light on the mathematical justification of other data-driven methods as well.

The remainder of the paper is organized as follows. In Section 2, we introduce chemical reaction networks and the required notation. In Section 3, we consider the learning of chemical

reaction networks from trajectory data and formulate it as an optimization problem. In Section 4, we demonstrate the efficiency of the numerical algorithm in solving the (sparse) optimization problems with three concrete numerical examples. In Section 5, we analyze the learning tasks when the length of the trajectory data goes to infinity and study the asymptotic behavior of the solutions of the optimization problems. Appendix A contains some properties of an elementary function, while two useful limit lemmas of counting processes are summarized in Appendix B.

The code used for producing the numerical results in Section 4 can be downloaded from: <https://github.com/zwpku/sparse-learning-CRN>.

2 Chemical reaction networks as continuous-time Markov chain: forward problem

Chemical reaction networks consist of different chemical species that can interact with each other through independent chemical reactions. Suppose that the system has n different chemical species, denoted by S_1, S_2, \dots, S_n . Each species S_i , $1 \leq i \leq n$, has $x^{(i)}$ copies, where the copy-number $x^{(i)} \geq 0$ may vary whenever a reaction involving the species S_i has occurred. The state of the system can be represented as the vector

$$x = (x^{(1)}, x^{(2)}, \dots, x^{(n)})^T \in \mathbb{X} \subseteq \mathbb{N}^n,$$

where $\mathbb{N} = \{0, 1, 2, \dots\}$ and \mathbb{X} is the set of all possible states of the system.

The evolution of the system’s state x can be modeled as a state-dependent continuous-time Markov chain [1, 19]. Let \mathcal{R} denote a reaction in the system. The state change vector v of \mathcal{R} , $v \in \mathbb{N}^n$, is defined such that, being at state x , the state of the system will change to $x + v$ when the reaction \mathcal{R} occurs. The waiting time $\tau_{\mathcal{R}}$ of the system before the reaction \mathcal{R} occurs obeys an exponential distribution with the rate parameter $a_{\mathcal{R}}^*(x)$ (propensity function), which in turn depends on both the state x and the structure of \mathcal{R} . Specifically, the probability density function of $\tau_{\mathcal{R}}$ is given by

$$\psi_{\mathcal{R}}^*(t | x) = a_{\mathcal{R}}^*(x) e^{-a_{\mathcal{R}}^*(x)t}, \quad t \geq 0.$$

In Table 1, we have listed the propensity functions of reactions which consume at most two molecules (see [24, 5] for further discussions). In particular, note that the propensity functions

Table 1: Propensity function $a_{\mathcal{R}}^*(x)$ as a function of the system’s state $x = (x^{(1)}, \dots, x^{(n)})^T$ for different types of chemical reactions. V is a constant related to either the volume or the total number of molecules in the system and κ denotes the rate constants of chemical reactions.

No.	Reaction \mathcal{R}	$a_{\mathcal{R}}^*(x)$
1	$\emptyset \xrightarrow{\kappa} \text{products}$	κV
2	$S_i \xrightarrow{\kappa} \text{products}$	$\kappa x^{(i)}$
3	$2 S_i \xrightarrow{\kappa} \text{products}$	$\frac{\kappa}{V} x^{(i)} (x^{(i)} - 1)$
4	$S_i + S_j \xrightarrow{\kappa} \text{products}$	$\frac{\kappa}{V} x^{(i)} x^{(j)}$

for the reactions in Table 1 are polynomial functions whose degrees are either 1 or 2.

In many reaction systems, different chemical reactions may have the same state change vector v . As a simple example, the state change vector of both reactions $A + B \longrightarrow B$ and $A \longrightarrow \emptyset$ is $v = (-1, 0)^T$. That is, the state of the system will change from $x = (x^{(1)}, x^{(2)})^T$ to $(x^{(1)} - 1, x^{(2)})^T$ when one of these two reactions occurs. Assume that N chemical reactions $\mathcal{R}_1, \mathcal{R}_2, \dots, \mathcal{R}_N$ are involved in the evolution of the system and these N reactions have in total K different state change vectors v_1, v_2, \dots, v_K , where $K \leq N$. For each vector v_i , $1 \leq i \leq K$, we introduce the terminology *chemical channel* \mathcal{C}_i . We say that the reaction \mathcal{R} belongs to the channel \mathcal{C}_i , or the channel \mathcal{C}_i contains the reaction \mathcal{R} , if the state change vector of \mathcal{R} is v_i . For each channel \mathcal{C}_i , we also define the set of indices

$$\mathcal{I}_i = \left\{ j \mid 1 \leq j \leq N, \mathcal{R}_j \text{ belongs to the channel } \mathcal{C}_i \right\},$$

and let N_i be the number of chemical reactions belonging to \mathcal{C}_i , i.e., $N_i = |\mathcal{I}_i|$. Clearly, these index sets satisfy

$$\bigcup_{i=1}^K \mathcal{I}_i = \{1, 2, \dots, N\}, \quad \text{and} \quad \mathcal{I}_i \cap \mathcal{I}_{i'} = \emptyset, \text{ if } i \neq i',$$

and therefore $\sum_{i=1}^K N_i = N$.

A reaction channel \mathcal{C}_i is said to be activated when a certain reaction \mathcal{R} belonging to \mathcal{C}_i occurs. For each $1 \leq i \leq K$, $\tau_i = \min_{j \in \mathcal{I}_i} \tau_{\mathcal{R}_j}$ is the waiting time at a state x before the activation of the channel \mathcal{C}_i , while

$$\tau = \min_{1 \leq j \leq N} \tau_{\mathcal{R}_j},$$

is the waiting time before any of the chemical reactions in the system occurs. Assuming the chemical reactions are independent of each other and the waiting times $\tau_{\mathcal{R}_j}$ follow exponential distributions, we know that the waiting times τ_i and τ also follow exponential distributions, with the propensity functions

$$a_i^*(x) = \sum_{j \in \mathcal{I}_i} a_{\mathcal{R}_j}^*(x), \quad a^*(x) = \sum_{i=1}^K a_i^*(x) = \sum_{j=1}^N a_{\mathcal{R}_j}^*(x), \quad (1)$$

respectively. In particular, let $\psi^*(t; x)$ be the probability density function of τ , and $p^*(i; x)$ be the probability that \mathcal{C}_i is the first channel which becomes activated at state x , then

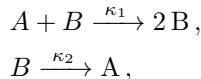
$$\begin{aligned} \psi^*(t; x) &= a^*(x) \exp(-a^*(x)t), \quad t \geq 0, \\ p^*(i; x) &= \frac{a_i^*(x)}{a^*(x)}, \quad 1 \leq i \leq K. \end{aligned} \quad (2)$$

Finally, let $X(t) \in \mathbb{N}^n$ denote the state of the system at time $t \geq 0$, from [1] we know that it satisfies the dynamical equation

$$X(t) = X(0) + \sum_{i=1}^K \mathcal{P}_i \left(\int_0^t a_i^*(X(s)) ds \right) v_i, \quad t \geq 0, \quad (3)$$

where \mathcal{P}_i are independent unit Poisson processes.

Remark 1. As a concrete example, let us consider a simple reaction network consisting of two species and two chemical reactions, given by



with rate constants $\kappa_1 = 0.1$ and $\kappa_2 = 1.0$. In this case, we have $N = K = 2$, since there are two reaction channels with state change vectors $v_1 = (-1, 1)^\top$ and $v_2 = (1, -1)^\top$. According to Table 1, the propensity functions of these two channels are (assuming $V = 1$)

$$a_1^*(x) = \kappa_1 x^{(1)} x^{(2)}, \quad a_2^*(x) = \kappa_2 x^{(2)},$$

respectively.

3 Learning chemical reaction networks: inverse problem

In this section, we study the problem of learning chemical reaction networks from trajectory data. Depending on the available information which is known about the chemical reaction networks, in Subsection 3.2 and Subsection 3.3 we consider two different learning tasks. In both tasks, the propensity functions in (1) are determined by maximizing the log-likelihood function among the parameterized propensity functions which depend on both a set of basis functions and several parameters. To emphasize the dependence on parameters, let the parameterized propensity functions be denoted by $a_i(x; \boldsymbol{\omega})$ and $a(x; \boldsymbol{\omega})$, respectively, where $x \in \mathbb{X}$ and $\boldsymbol{\omega}$ is the vector consisting of all parameters. Similar to (2), we define the probability (density) functions corresponding to $\boldsymbol{\omega}$

$$\begin{aligned} \psi(t; x, \boldsymbol{\omega}) &= a(x; \boldsymbol{\omega}) \exp(-a(x; \boldsymbol{\omega})t), \quad t \geq 0, \\ p(i; x, \boldsymbol{\omega}) &= \frac{a_i(x; \boldsymbol{\omega})}{a(x; \boldsymbol{\omega})}, \quad 1 \leq i \leq K. \end{aligned} \tag{4}$$

In the first learning task (Subsection 3.2), we assume that the structures of the chemical reactions are known and the goal is to determine the reaction rate constant of each reaction, i.e., the constants κ in Table 1. In this case, each basis function in the parameterized propensity functions corresponds to an actual chemical reaction that is indeed involved in the evolution of the system (no redundancy), while the task is to determine the value of each parameter (parameter estimation). In the second learning task (Subsection 3.3), on the other hand, we assume that the structures of the chemical reactions in the system are also unknown. In this case, candidate basis functions are chosen to parameterize the propensity functions, and l^1 sparsity regularization is used to remove the redundancy in the basis functions.

Before introducing the two learning tasks, in Subsection 3.1 we first present a brief discussion on the trajectory of the system and particularly the likelihood function of a given trajectory will be derived.

3.1 Space of trajectories and the likelihood function

Given $T > 0$, there are two different ways to represent the trajectories of the system within the time $[0, T]$. The first representation relies on the total number M of reactions occurred

within $[0, T]$, the waiting time τ of each reaction, and the new state of the system after each of the M reactions. Specifically, starting from a state $y_0 \in \mathbb{X}$ at time $s = 0$, each trajectory $X(s)$ in the time $[0, T]$ can be represented as the sequence

$$(y_0, t_0), (y_1, t_1), (y_2, t_2), \dots, (y_M, t_M), \quad (5)$$

which means that, starting from y_0 , the state of the system changes from y_l to y_{l+1} after waiting for a period of time of length t_l , where $0 \leq l < M$. The final time t_M in (5) is the amount of time that the system spends at the final state y_M before time $s = T$. Clearly, we have

$$\sum_{l=0}^M t_l = T.$$

In the second representation, the indices of reaction channels are used instead of system's new state after each reaction. That is, we represent the same trajectory $X(s)$, $s \in [0, T]$, as

$$(i_0, t_0), (i_1, t_1), (i_2, t_2), \dots, (i_{M-1}, t_{M-1}), \quad (6)$$

where, for each $0 \leq l < M$, $i_l \in \{1, 2, \dots, K\}$ denotes the index of the reaction channel and $t_l > 0$ is the waiting time before the $(l+1)$ -th reaction occurs, respectively. The two representations (5) and (6) can be converted from one to the other, using the relation $v_{i_l} = y_{l+1} - y_l$, which holds for $0 \leq l < M$.

In this work, we suppose that a trajectory $X(s)$ of the system, represented either as described in (5) or (6), is available up to time T . In other words, we assume that both the change of the state and the length of the waiting time are known for each occurrence of the M chemical reactions. From the trajectory data, we can deduce the total number of different reaction channels K , as well as the state change vector $v_i \in \mathbb{N}^n$ for each channel \mathcal{C}_i , $1 \leq i \leq K$. (Note, however, that when a certain channel \mathcal{C} contains more than one reaction, from the data alone we will not be able to tell which reaction \mathcal{R} belonging to \mathcal{C} has actually occurred when \mathcal{C} is activated.) For each $1 \leq i \leq K$, we denote by

$$0 \leq l_1^{(i)} < l_2^{(i)} < \dots < l_{M_i}^{(i)} < M, \quad (7)$$

the indices l such that $i_l = i$ in (6), where $M_i \geq 0$ is the total number that the channel \mathcal{C}_i has been activated within time $[0, T]$, and therefore the relation

$$\sum_{i=1}^K M_i = M \quad (8)$$

is satisfied.

For brevity, let us introduce the notation

$$\mathbf{X} = \left(M, (y_l, t_l)_{l=0,1,\dots,M} \right) \quad (9)$$

to describe the trajectory of the system within the time interval $[0, T]$. The space consisting of all trajectories of the system on $[0, T]$ will be denoted by \mathcal{D}_T . Note that, as a random variable, \mathbf{X} contains both continuous and discrete components. Given a parameter vector ω , we consider

the chemical reaction system determined by the (parameterized) probability density functions ψ , p in (4), and define

$$\rho^{(T)}(\mathbf{X}|\boldsymbol{\omega}) = \left[\prod_{l=0}^{M-1} \psi(t_l; y_l, \boldsymbol{\omega}) p(i_l; y_l, \boldsymbol{\omega}) \right] \exp \left(-a(y_M; \boldsymbol{\omega}) t_M \right), \quad (10)$$

for the trajectory \mathbf{X} in (9). Let \mathbf{E} denote the mathematical expectation with respect to the trajectories of the system. Then, for any bounded measurable function $g: \mathcal{D}_T \rightarrow \mathbb{R}$, we have

$$\mathbf{E}g(\mathbf{X}) = \sum_{M=0}^{+\infty} \sum_{i_0=1}^K \sum_{i_1=1}^K \cdots \sum_{i_{M-1}=1}^K \int_{\{t_0+t_1+\cdots+t_M=T\}} g(\mathbf{X}) \rho^{(T)}(\mathbf{X}|\boldsymbol{\omega}) dt_0 dt_1 \cdots dt_{M-1}, \quad (11)$$

from which we can view the function $\rho^{(T)}(\mathbf{X}|\boldsymbol{\omega})$ as the probability density (distribution) of \mathbf{X} on the space \mathcal{D}_T (we can indeed verify that $\mathbf{E}1 = 1$). To simplify the notation, we will formally write

$$\mathbf{E}g(\mathbf{X}) = \int_{\mathcal{D}_T} g(\mathbf{X}) \rho^{(T)}(\mathbf{X}|\boldsymbol{\omega}) d\mathbf{X} \quad (12)$$

as the integration on the right hand side of (11).

From (10) and (12), we can write down the likelihood function of the trajectory data as

$$\begin{aligned} \mathcal{L}^{(T)}(\boldsymbol{\omega}) &= \mathcal{L}^{(T)}(\boldsymbol{\omega} | \mathbf{X}) \\ &= \rho^{(T)}(\mathbf{X}|\boldsymbol{\omega}) \\ &= \left[\prod_{l=0}^{M-1} \psi(t_l; y_l, \boldsymbol{\omega}) p(i_l; y_l, \boldsymbol{\omega}) \right] \exp \left(-a(y_M; \boldsymbol{\omega}) t_M \right) \\ &= \left[\prod_{l=0}^M \exp \left(-a(y_l; \boldsymbol{\omega}) t_l \right) \right] \prod_{l=0}^{M-1} a_{i_l}(y_l; \boldsymbol{\omega}) \\ &= \prod_{i=1}^K \mathcal{L}_i^{(T)}(\boldsymbol{\omega}), \end{aligned} \quad (13)$$

where

$$\mathcal{L}_i^{(T)}(\boldsymbol{\omega}) = \left[\prod_{l=0}^M \exp \left(-a_i(y_l; \boldsymbol{\omega}) t_l \right) \right] \prod_{k=1}^{M_i} a_i(y_{l_k^{(i)}}; \boldsymbol{\omega}), \quad 1 \leq i \leq K, \quad (14)$$

can be considered as the likelihood function along the reaction channel \mathcal{C}_i .

3.2 Learning task 1: Determine rate constants by maximizing the log-likelihood

Assuming that the structures of the chemical reactions in the system are known, in this subsection we study the problem of determining the reaction rate constant of each reaction. Note that the propensity function of each reaction \mathcal{R} in Table 1 can be written as $\omega\varphi(x)$, where $\varphi(x)$ is a polynomial of the system's state whose specific form depends on the structure of \mathcal{R} , and ω is the rate constant. Therefore, in the current learning task we assume that the propensity function of the j th chemical reaction \mathcal{R}_j in the system is given by

$$a_{\mathcal{R}_j}^*(x) = \omega_j \varphi_j(x), \quad 1 \leq j \leq N, \quad (15)$$

where the nonnegative function φ_j is known from the structure of \mathcal{R}_j , and ω_j is the unknown rate constant which we want to determine from trajectory data.

Let $\boldsymbol{\omega}$ be the vector

$$\boldsymbol{\omega} = (\omega_1, \omega_2, \dots, \omega_N)^T \in \mathbb{R}^N, \quad (16)$$

consisting of all the unknown rate constants, where $\omega_j \geq 0$ for all $1 \leq j \leq N$. For each channel \mathcal{C}_i , $1 \leq i \leq K$, we also define the vector

$$\boldsymbol{\omega}^{(i)} = (\omega_{j_1}, \omega_{j_2}, \dots, \omega_{j_{N_i}})^T, \quad \text{where } \mathcal{I}_i = \{j_1, j_2, \dots, j_{N_i}\},$$

which consists of the rate constants of reactions belonging to \mathcal{C}_i . Corresponding to (15), the parameterized propensity functions in (1) are

$$\begin{aligned} a_i(x; \boldsymbol{\omega}) &= a_i(x; \boldsymbol{\omega}^{(i)}) = \sum_{j \in \mathcal{I}_i} \omega_j \varphi_j(x), \quad 1 \leq i \leq K, \\ \text{and } a(x; \boldsymbol{\omega}) &= \sum_{j=1}^N \omega_j \varphi_j(x), \end{aligned} \quad (17)$$

while the optimal value of $\boldsymbol{\omega}$ is determined by maximizing the (logarithmic) likelihood functions in (13), or equivalently, by solving the minimization problem

$$\min_{\boldsymbol{\omega}} \left[-\ln \mathcal{L}^{(T)}(\boldsymbol{\omega}) \right]. \quad (18)$$

With the trajectory data as defined in (5) and using the propensity functions in (17), the objective function above can be computed explicitly and we have

$$\begin{aligned} & -\ln \mathcal{L}^{(T)}(\boldsymbol{\omega}) \\ &= -\sum_{l=0}^{M-1} \ln \left[\sum_{j \in \mathcal{I}_l} \omega_j \varphi_j(y_l) \right] + \sum_{l=0}^M t_l \left[\sum_{j=1}^N \omega_j \varphi_j(y_l) \right] \\ &= -\sum_{i=1}^K \sum_{k=1}^{M_i} \ln \left[\sum_{j \in \mathcal{I}_i} \omega_j \varphi_j(y_{l_k^{(i)}}) \right] + \sum_{l=0}^M t_l \left[\sum_{j=1}^N \omega_j \varphi_j(y_l) \right] \\ &= -\sum_{i=1}^K \ln \mathcal{L}_i^{(T)}(\boldsymbol{\omega}^{(i)}), \end{aligned} \quad (19)$$

where we recall that the indices $l_k^{(i)}$ are defined in (7), the logarithmic likelihood function

$$\ln \mathcal{L}_i^{(T)}(\boldsymbol{\omega}^{(i)}) = \sum_{k=1}^{M_i} \ln \left[\sum_{j \in \mathcal{I}_i} \omega_j \varphi_j(y_{l_k^{(i)}}) \right] - \sum_{l=0}^M t_l \left[\sum_{j \in \mathcal{I}_i} \omega_j \varphi_j(y_l) \right] \quad (20)$$

only depends on $\boldsymbol{\omega}^{(i)}$ and should be compared to (14). Note that the above expressions also imply that the minimization problem (18) can be decomposed into K minimization problems

$$\min_{\boldsymbol{\omega}^{(i)}} \left[-\ln \mathcal{L}_i^{(T)}(\boldsymbol{\omega}^{(i)}) \right], \quad 1 \leq i \leq K,$$

which can be solved separately.

For each index j , $1 \leq j \leq N$, such that $j \in \mathcal{I}_i$ for some $1 \leq i \leq K$, the corresponding Euler–Lagrange equation of (18) is

$$\mathcal{M}_j^{(T)}(\omega) = \frac{\partial(-\ln \mathcal{L}^{(T)})}{\partial \omega_j}(\omega) = - \sum_{k=1}^{M_i} \frac{\varphi_j(y_{l_k^{(i)}})}{\sum_{j' \in \mathcal{I}_i} \omega_{j'} \varphi_{j'}(y_{l_k^{(i)}})} + \sum_{l=0}^M t_l \varphi_j(y_l) = 0. \quad (21)$$

Differentiating one more time, we get the Hessian matrix of the objective function in (18)

$$\frac{\partial^2(-\ln \mathcal{L}^{(T)})}{\partial \omega_j \partial \omega_{j'}}(\omega) = \frac{\partial \mathcal{M}_j^{(T)}}{\partial \omega_{j'}}(\omega) = \begin{cases} \sum_{k=1}^{M_i} \frac{\varphi_j(y_{l_k^{(i)}}) \varphi_{j'}(y_{l_k^{(i)}})}{\left(\sum_{r \in \mathcal{I}_i} \omega_r \varphi_r(y_{l_k^{(i)}})\right)^2}, & \text{if } j, j' \in \mathcal{I}_i, \\ 0, & \text{otherwise,} \end{cases} \quad (22)$$

where $1 \leq j, j' \leq N$.

In order to study the optimization problem (18)–(19), let us introduce the matrix

$$\Phi_i = \begin{bmatrix} \varphi_{j_1}(y_{l_1^{(i)}}) & \varphi_{j_2}(y_{l_1^{(i)}}) & \cdots & \varphi_{j_{N_i}}(y_{l_1^{(i)}}) \\ \varphi_{j_1}(y_{l_2^{(i)}}) & \varphi_{j_2}(y_{l_2^{(i)}}) & \cdots & \varphi_{j_{N_i}}(y_{l_2^{(i)}}) \\ \varphi_{j_1}(y_{l_3^{(i)}}) & \varphi_{j_2}(y_{l_3^{(i)}}) & \cdots & \varphi_{j_{N_i}}(y_{l_3^{(i)}}) \\ \vdots & \vdots & \ddots & \vdots \\ \varphi_{j_1}(y_{l_{M_i}^{(i)}}) & \varphi_{j_2}(y_{l_{M_i}^{(i)}}) & \cdots & \varphi_{j_{N_i}}(y_{l_{M_i}^{(i)}}) \end{bmatrix} \in \mathbb{R}^{M_i \times N_i}, \quad (23)$$

for each $1 \leq i \leq K$, where we have assumed that the index set $\mathcal{I}_i = \{j_1, j_2, \dots, j_{N_i}\}$. Also define by $\Phi_{i,k} \in \mathbb{R}^{M_i}$ the k th column vector of Φ_i for $1 \leq k \leq N_i$. We obtain the following result concerning the solution of the optimization problem (18)–(19).

Proposition 1. *The following three conditions are equivalent.*

- (1) *For each $1 \leq i \leq K$, vectors $\Phi_{i,1}, \Phi_{i,2}, \dots, \Phi_{i,N_i}$ are linearly independent.*
- (2) *The function $-\ln \mathcal{L}^{(T)}(\omega)$ in (19) is strictly convex.*
- (3) *The optimization problem (18)–(19) has a unique solution.*

Proof. (2) \Rightarrow (3) is obvious. To show that (1) implies (2), it is sufficient to verify that the Hessian matrix of $-\ln \mathcal{L}^{(T)}$ is positive definite. Using (22), for any vector $\boldsymbol{\eta} = (\eta_1, \eta_2, \dots, \eta_N)^T \in \mathbb{R}^N$, we have

$$\sum_{j=1}^N \sum_{j'=1}^N \frac{\partial^2(-\ln \mathcal{L}^{(T)})}{\partial \omega_j \partial \omega_{j'}} \eta_j \eta_{j'} = \sum_{i=1}^K \sum_{k=1}^{M_i} \frac{\left(\sum_{j \in \mathcal{I}_i} \eta_j \varphi_j(y_{l_k^{(i)}})\right)^2}{\left(\sum_{j \in \mathcal{I}_i} \omega_j \varphi_j(y_{l_k^{(i)}})\right)^2} \geq 0. \quad (24)$$

Since the columns of Φ_i are linearly independent for each i , we conclude that (24) is zero if and only if $\boldsymbol{\eta}$ is a zero vector. This implies that $-\ln \mathcal{L}^{(T)}$ is strictly convex.

Finally, let us prove that (3) implies (1) by contradiction. Define ω to be the unique solution of the optimization problem (18). Assume that there is i , $1 \leq i \leq K$, such that

the vectors $\Phi_{i,1}, \Phi_{i,2}, \dots, \Phi_{i,N_i}$ are linearly dependent. As a result, we can find a vector $\tilde{\omega} = (\tilde{\omega}_1, \tilde{\omega}_2, \dots, \tilde{\omega}_N)^T \neq \omega$, such that

$$\begin{aligned} \tilde{\omega}_j &= \omega_j, & \forall j \in \mathcal{I}_{i'}, i' \neq i, \\ \text{and } \sum_{j \in \mathcal{I}_i} \tilde{\omega}_j \varphi_j(y_{l_k^{(i)}}) &= \sum_{j \in \mathcal{I}_i} \omega_j \varphi_j(y_{l_k^{(i)}}), & \forall 1 \leq k \leq M_i. \end{aligned} \quad (25)$$

Since ω satisfies the Euler–Lagrange equation (21), the property (25) implies that $\tilde{\omega}$ satisfies (21) as well. Multiplying by ω_j (or $\tilde{\omega}_j$) on both sides of (21) and summing up the indices, we get

$$\sum_{l=0}^M t_l \left[\sum_{j=1}^N \tilde{\omega}_j \varphi_j(y_l) \right] = \sum_{l=0}^M t_l \left[\sum_{j=1}^N \omega_j \varphi_j(y_l) \right] = M. \quad (26)$$

Combining (25), (26), as well as the expressions in (19), we obtain that $-\ln \mathcal{L}^{(T)}(\omega) = -\ln \mathcal{L}^{(T)}(\tilde{\omega})$, which contradicts the uniqueness of ω . \square

To distinguish the parameters obtained from solving the optimization problem (18) and the true parameters of the system, in what follow, we will define $\omega^{(T)}$ to be the maximizer of $-\ln \mathcal{L}^{(T)}$ for fixed time $T > 0$, and ω^* to be the vector consisting of the true parameters such that (15) holds. In particular, when $N_i = 1$ and $\mathcal{I}_i = \{j\}$, i.e., the channel \mathcal{C}_i only contains one reaction \mathcal{R}_j , the Euler–Lagrange equation (21) can be solved analytically and we have

$$\omega_j^{(T)} = \frac{M_i}{\sum_{l=0}^M t_l \varphi_j(y_l)}. \quad (27)$$

3.3 Learning task 2: Determine both rate constants and the structure of chemical reactions using sparsity

In this subsection, we study the problem of learning the propensity functions of the chemical reaction networks from trajectory data when neither the structures of the chemical reactions nor their rate constants are known.

First of all, we can figure out the total number K of the reaction channels from the trajectory data, as discussed in Subsection 3.1. Now suppose that we are given N candidate basis functions

$$\varphi_j : \mathbb{N}^n \rightarrow \mathbb{R}, \quad 1 \leq j \leq N, \quad (28)$$

together with K index sets $\mathcal{I}_i = \{j_1, j_2, \dots, j_{N_i}\}$, $1 \leq i \leq K$, such that $N_i = |\mathcal{I}_i|$,

$$\bigcup_{i=1}^K \mathcal{I}_i = \{1, 2, \dots, N\}, \quad \text{and} \quad \mathcal{I}_i \cap \mathcal{I}_{i'} = \emptyset, \text{ if } i \neq i'. \quad (29)$$

Accordingly, we introduce the vectors

$$\omega = (\omega_1, \omega_2, \dots, \omega_N)^T \in \mathbb{R}^N, \quad \text{and} \quad \omega^{(i)} = (\omega_{j_1}, \omega_{j_2}, \dots, \omega_{j_{N_i}})^T \in \mathbb{R}^{N_i}. \quad (30)$$

For each channel \mathcal{C}_i , the propensity function a_i^* in (1) will be approximated using the basis functions φ_j , $j \in \mathcal{I}_i$, and the coefficients in $\omega^{(i)}$. More precisely, we define

$$a_i^{(\epsilon)}(x; \omega) = a_i^{(\epsilon)}(x; \omega^{(i)}) = G_\epsilon \left(\sum_{j \in \mathcal{I}_i} \omega_j \varphi_j(x) \right), \quad (31)$$

where $\epsilon > 0$, and the function

$$G_\epsilon(x) = \epsilon \ln(1 + e^{x/\epsilon}), \quad \epsilon > 0, \quad (32)$$

is introduced (see Figure 1), in order to guarantee the nonnegativity of $a_i^{(\epsilon)}$ for all vectors $\boldsymbol{\omega} \in \mathbb{R}^N$. Corresponding to (31), the total propensity function is given by

$$a^{(\epsilon)}(x; \boldsymbol{\omega}) = \sum_{i=1}^K G_\epsilon \left(\sum_{j \in \mathcal{I}_i} \omega_j \varphi_j(x) \right). \quad (33)$$

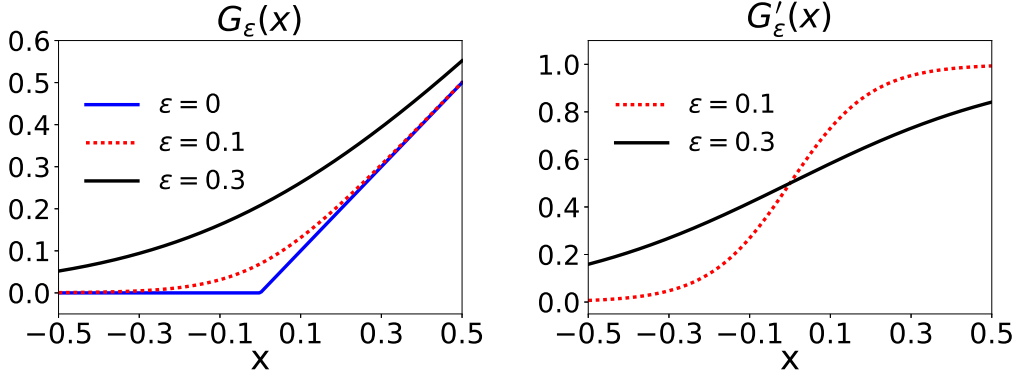


Figure 1: Profiles of G_ϵ in (32) and its derivative G'_ϵ . For $\epsilon = 0$, we define $G_0(x) = \lim_{\epsilon \rightarrow 0+} G_\epsilon(x) = \max(x, 0)$. See Remark 2 and Appendix A for the properties of G_ϵ as $\epsilon \rightarrow 0+$.

Since the propensity functions of reactions in many applications typically have a simple form (Table 1), there is likely redundancy in the basis functions and therefore we can assume that the unknown vector $\boldsymbol{\omega}$ only has a few nonzero entries (and is thus sparse). With this observation in mind, we propose to determine $\boldsymbol{\omega}$ by maximizing the (logarithmic) likelihood function under the sparsity assumption, or, equivalently, by solving the nonlinear sparsity minimization problem

$$\min_{\boldsymbol{\omega}} \left[-\ln \mathcal{L}^{(T, \epsilon)}(\boldsymbol{\omega}) \right], \quad \boldsymbol{\omega} \text{ is sparse}, \quad (34)$$

where $\mathcal{L}^{(T, \epsilon)}(\boldsymbol{\omega})$ is the likelihood function (13) with the propensity functions $a_i = a_i^{(\epsilon)}$, $a = a^{(\epsilon)}$ in (31), (33). Explicitly, we have

$$\begin{aligned} & -\ln \mathcal{L}^{(T, \epsilon)}(\boldsymbol{\omega}) \\ &= -\sum_{l=0}^{M-1} \ln G_\epsilon \left(\sum_{j \in \mathcal{I}_{i_l}} \omega_j \varphi_j(y_l) \right) + \sum_{l=0}^M t_l \left[\sum_{i=1}^K G_\epsilon \left(\sum_{j \in \mathcal{I}_i} \omega_j \varphi_j(y_l) \right) \right]. \end{aligned} \quad (35)$$

If we quantify the sparsity of $\boldsymbol{\omega}$ using the l^1 norm (denoted by $\|\cdot\|_1$), then (34) results in

$$\min_{\boldsymbol{\omega}} \left(-\frac{1}{T} \ln \mathcal{L}^{(T, \epsilon)}(\boldsymbol{\omega}) + \lambda \|\boldsymbol{\omega}\|_1 \right). \quad (36)$$

In (36), the log-likelihood function is rescaled by $1/T$ (this scaling is suggested by the analysis in Section 5), and the constant $\lambda = \lambda(T) > 0$, which measures the strength of the sparsity regularization, can be chosen depending on T .

Similar to the problem (18) in the previous subsection, the minimizer of (36) can be computed by solving K sparse minimization problems

$$\min_{\omega^{(i)}} \left(-\frac{1}{T} \ln \mathcal{L}_i^{(T,\epsilon)}(\omega^{(i)}) + \lambda \|\omega^{(i)}\|_1 \right), \quad 1 \leq i \leq K, \quad (37)$$

separately, where

$$\ln \mathcal{L}_i^{(T,\epsilon)}(\omega^{(i)}) = \sum_{k=1}^{M_i} \ln G_\epsilon \left(\sum_{j \in \mathcal{I}_i} \omega_j \varphi_j(y_{l_k^{(i)}}) \right) - \sum_{l=0}^M t_l G_\epsilon \left(\sum_{j \in \mathcal{I}_i} \omega_j \varphi_j(y_l) \right). \quad (38)$$

Remark 2. Several remarks are in order:

1. The properties of the function G_ϵ in (32) are provided in Appendix A. In particular, we have $\lim_{\epsilon \rightarrow 0+} G_\epsilon(x) = \max(x, 0)$, uniformly for all $x \in \mathbb{R}$. For this reason, we will use the convention that $G_0(x) = \max(x, 0)$.
2. In the sparse minimization problem (36), the vector ω contains all the N coefficients ω_j , and the corresponding N basis functions φ_j in (28) are involved. This formulation makes the notations simpler and is also convenient for analysis, particularly in Section 5. Numerically, on the other hand, the coefficient vectors $\omega^{(i)}$ in (30) are computed separately by solving the minimization problems (37), $1 \leq i \leq K$, with the same set of basis functions $\phi_1, \phi_2, \dots, \phi_L$, $L > 0$, for all the K channels. In this case, corresponding to the formulation adopted at the beginning of this subsection where all N coefficients are put together, we can define the index sets

$$\mathcal{I}_i = \left\{ (i-1)L + 1, (i-1)L + 2, \dots, iL \right\}, \quad 1 \leq i \leq K,$$

and for each $j \in \mathcal{I}_i$, we define the function

$$\varphi_j = \phi_k, \quad \text{when } j = (i-1)L + k, \quad 1 \leq k \leq L. \quad (39)$$

Accordingly, we have

$$\omega^{(i)} = (\omega_{(i-1)L+1}, \omega_{(i-1)L+2}, \dots, \omega_{(i-1)L+L})^T,$$

and the propensity function in (31) can be written more transparently as

$$a_i^{(\epsilon)}(x; \omega) = a_i^{(\epsilon)}(x; \omega^{(i)}) = G_\epsilon \left(\sum_{k=1}^L \omega_{(i-1)L+k} \phi_k(x) \right).$$

3. While we are mainly interested in chemical reaction systems, the same learning approach can be applied to other types of continuous-time Markov chains whose jump distributions are state-dependent. In particular, for chemical reaction systems, we may choose φ_j as polynomials according to Table 1

$$\begin{aligned} & 1, \quad x^{(1)}, \quad x^{(2)}, \quad \dots, \quad x^{(n)}, \\ & x^{(1)}x^{(2)}, \quad x^{(1)}x^{(3)}, \quad \dots, \quad x^{(1)}x^{(n)}, \quad x^{(2)}x^{(3)}, \quad \dots, \quad x^{(n-1)}x^{(n)}, \\ & \dots, \end{aligned}$$

where $x^{(k)}$ denotes the k th component of the state $x = (x^{(1)}, x^{(2)}, \dots, x^{(n)})^T$, based on the knowledge about the potential chemical reactions that are possibly involved in the system.

4. In concrete applications, due to the complexity of the trajectory data, different basis functions may take values that are of different orders of magnitude. As a result, the objective functions in (37), or equivalently in (36), may become inhomogeneous along different components ω_j . This leads to numerical difficulties in solving (37), since a small step-size has to be used as a result of the strong dependence of the objective function on the change of ω along certain directions (i.e., large gradient, ill-conditioned). A simple way to alleviate this numerical issue is to precondition the problems (37) by rescaling the basis functions. Equivalently, let c_j denote the rescaling constants, where $c_j > 0$, $1 \leq j \leq N$. Instead of (37), we can solve the minimizer $\bar{\omega}^{(i)}$ of the rescaled sparse minimization problem

$$\min_{\bar{\omega}^{(i)}} \left\{ -\frac{1}{T} \sum_{k=1}^{M_i} \ln G_\epsilon \left(\sum_{j \in \mathcal{I}_i} \frac{\bar{\omega}_j}{c_j} \varphi_j(y_{l_k^{(i)}}) \right) + \frac{1}{T} \sum_{l=0}^M t_l G_\epsilon \left(\sum_{j \in \mathcal{I}_i} \frac{\bar{\omega}_j}{c_j} \varphi_j(y_l) \right) + \lambda \sum_{j \in \mathcal{I}_i} \frac{|\bar{\omega}_j|}{c_j} \right\}, \quad (40)$$

where the vector $\bar{\omega}^{(i)}$ consists of $\bar{\omega}_j$, $j \in \mathcal{I}_i$. Then, it is easy to verify that the minimizer $\omega^{(i)}$ of (37) can be recovered from $\omega_j = \frac{\bar{\omega}_j}{c_j}$, for $j \in \mathcal{I}_i$. By properly choosing the constants c_j based on analyzing the trajectory data, we can expect that minimizing (40) will be easier compared to (37). Readers are referred to Section 4 for further discussions on this issue and concrete examples.

We obtain the following result concerning the minimization problems (36) and (37).

Proposition 2. Suppose $\epsilon, \lambda > 0$. The objective functions of the optimization problems (36) and (37) are strictly convex.

Proof. It is sufficient to consider the objective function in (37). By straightforward calculations (for instance, see (88) and (89) in Appendix A), we can verify that both $-\ln G_\epsilon$ and G_ϵ are strictly convex functions. Therefore, the function $-\ln \mathcal{L}_i^{(T, \epsilon)}$ in (38) is strictly convex. Since the norm $\|\cdot\|_1$ is convex as well, we conclude that the objective function in (37) is strictly convex. \square

Let $\omega^{(T, \epsilon, \lambda)}$ denote the unique minimizer of the problem (36). Similar to the Euler–Lagrange equation (21), in the current case $\omega^{(T, \epsilon, \lambda)}$ satisfies the inclusion relation [4, 12]

$$\frac{1}{T} \mathcal{M}_j^{T, \epsilon}(\omega) \in -\lambda \partial |\omega_j|, \quad \forall 1 \leq j \leq N, \quad (41)$$

where

$$\begin{aligned} \mathcal{M}_j^{(T, \epsilon)}(\omega) &= \frac{\partial(-\ln \mathcal{L}^{(T, \epsilon)})}{\partial \omega_j}(\omega) \\ &= -\sum_{k=1}^{M_i} \frac{G'_\epsilon \left(\sum_{j' \in \mathcal{I}_i} \omega_{j'} \varphi_{j'}(y_{l_k^{(i)}}) \right) \varphi_j(y_{l_k^{(i)}})}{G_\epsilon \left(\sum_{j' \in \mathcal{I}_i} \omega_{j'} \varphi_{j'}(y_{l_k^{(i)}}) \right)} + \sum_{l=0}^M t_l \left[G'_\epsilon \left(\sum_{j' \in \mathcal{I}_i} \omega_{j'} \varphi_{j'}(y_l) \right) \varphi_j(y_l) \right], \end{aligned} \quad (42)$$

for $j \in \mathcal{I}_i$, and $\partial |\omega_j|$ is the subdifferential of the absolute value function $|\omega_j|$, defined by

$$\partial |\omega_j| = \begin{cases} \{1\}, & \omega_j > 0, \\ [-1, 1], & \omega_j = 0, \\ \{-1\}, & \omega_j < 0. \end{cases}$$

Finally, let $\mathcal{M}^{(T,\epsilon)}$ be the vector in \mathbb{R}^N whose components are in (42) and define the set

$$\partial|\omega| = \left\{ \mathbf{v} \in \mathbb{R}^N \mid \mathbf{v} = (v_1, v_2, \dots, v_N)^T, v_j \in \partial|\omega_j|, 1 \leq j \leq N \right\}.$$

We can express the condition (41) in the vector form as

$$\frac{1}{T} \mathcal{M}^{T,\epsilon}(\omega) \in -\lambda \partial|\omega|. \quad (43)$$

The above characterization of the minimizers will be used in the analysis in Section 5.

4 Examples

In this section, we study the learning tasks discussed in Section 3 with three concrete numerical examples.

4.1 Example 1

In the first example, we study the chemical reaction system in Table 2, where 2 different species A, B are involved in 4 chemical reactions. The propensity functions of these 4 reactions depend on both the system's state $x = (x^{(1)}, x^{(2)})^T$, i.e., the copy-numbers of the species A and B , and the rate constants κ_i , $i = 1, 2, 3, 4$.

To study the two learning tasks discussed in Section 3, we fix the parameters

$$(\kappa_1, \kappa_2, \kappa_3, \kappa_4) = (1.0, 0.1, 1.0, 0.9), \quad (44)$$

and $Q = 100$ trajectories of the system are generated using the stochastic simulation algorithm (SSA) [17, 18, 19]. Each trajectory starts from the same initial state $x = (20, 10)^T$ at time $t = 0$ and is simulated until time $T = 10$ (5 of the 100 trajectories are shown in Figure 2 for illustration). From Table 2, it is clear that different reactions belong to different reaction channels and therefore there are in total 4 reaction channels in the reaction network. For the quantities introduced in Section 2, we have that $N_i = 1$ and $K = N = 4$. After processing the trajectory data, we find that the activation numbers of the 4 reaction channels within these 100 trajectories are 2296, 1778, 2777, and 2135, respectively, as shown in Table 3.

Table 2: Example 1. Chemical reaction system consists of 2 species A and B and 4 chemical reactions. The copy-numbers of these 2 species are denoted by $x = (x^{(1)}, x^{(2)})^T$. Here, κ_i , v , and $a_{\mathcal{R}}^*(x)$ are the rate constant, the state change vector, and the propensity function of the reactions, respectively.

No.	Reaction	v^T	Channel	$a_{\mathcal{R}}^*(x)$
1	$A \xrightarrow{\kappa_1} \emptyset$	$(-1, 0)$	1	$\kappa_1 x^{(1)}$
2	$A + B \xrightarrow{\kappa_2} 2B$	$(-1, 1)$	2	$\kappa_2 x^{(1)} x^{(2)}$
3	$B \xrightarrow{\kappa_3} \emptyset$	$(0, -1)$	3	$\kappa_3 x^{(2)}$
4	$A \xrightarrow{\kappa_4} 2A$	$(1, 0)$	4	$\kappa_4 x^{(1)}$

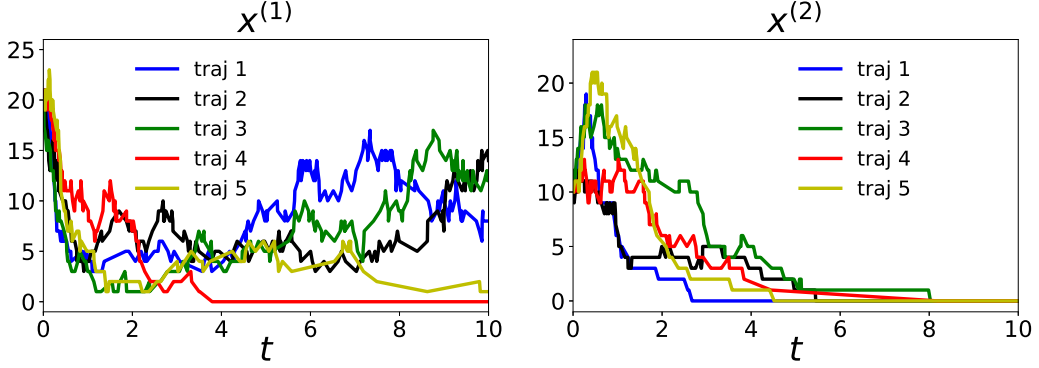


Figure 2: Example 1. The evolution of the system's state $x = (x^{(1)}, x^{(2)})^T$. Displayed are 5 sample trajectories (of overall 100 trajectories).

With the prepared trajectory data, let us first consider the problem of learning the rate constants κ_i , $1 \leq i \leq 4$, assuming that the types of these 4 reactions are known. For this purpose, we consider the negative log-likelihood function

$$\begin{aligned}
& -\frac{1}{QT} \ln \mathcal{L}^{(T)}(\omega) \\
&= -\frac{1}{QT} \sum_{q=1}^Q \left\{ \sum_{l=0}^{M^{(q)}-1} \ln \left[\sum_{j \in \mathcal{I}_{i_l^{(q)}}} \omega_j \varphi_j(y_l^{(q)}) \right] + \sum_{l=0}^{M^{(q)}} t_l^{(q)} \left[\sum_{j=1}^N \omega_j \varphi_j(y_l^{(q)}) \right] \right\} \\
&= -\frac{1}{QT} \sum_{q=1}^Q \sum_{i=1}^K \left\{ \sum_{k=1}^{M_i^{(q)}} \ln \left[\sum_{j \in \mathcal{I}_i} \omega_j \varphi_j(y_{l_k^{(q,i)}}^{(q)}) \right] + \sum_{l=0}^{M^{(q)}} t_l^{(q)} \left[\sum_{j \in \mathcal{I}_i} \omega_j \varphi_j(y_l^{(q)}) \right] \right\},
\end{aligned} \tag{45}$$

which is similar to (19), except that in (45) we have taken all the 100 trajectories into account. Specifically, q in (45) denotes the index of the trajectory, while the notation $M^{(q)}$, $M_i^{(q)}$, $i_l^{(q)}$, $y_l^{(q)}$, $t_l^{(q)}$, $l_k^{(q,i)}$ has the same meaning (for the q th trajectory) as the corresponding notations M , M_i , i_l , y_l , t_l , and $l_k^{(i)}$ in (19), respectively. Following the setting in Subsection 3.2, in this example we have the parameter set $\omega = (\kappa_1, \kappa_2, \kappa_3, \kappa_4)^T$, the index set $\mathcal{I}_i = \{i\}$, $1 \leq i \leq 4$, as well as the functions given by

$$\varphi_1(x) = x^{(1)}, \quad \varphi_2(x) = x^{(1)}x^{(2)}, \quad \varphi_3(x) = x^{(2)}, \quad \varphi_4(x) = x^{(1)}.$$

Since each reaction channel only contains one single reaction, the minimizer of the objective function (45) can be computed explicitly using an expression similar to (27), and we get

$$\omega^{(T)} = (0.98, 0.10, 0.97, 0.91)^T,$$

which is indeed close to the true parameters (see Table 4).

Let us now study the second learning task in Subsection 3.3 with the same trajectory data, where we assume that the structure of the chemical reactions involved in the system is unknown as well. Notice that, by analyzing the trajectory data, in this case we can still figure out that there are in total 2 species and 4 different reaction channels in the reaction network (see Table 3).

In order to determine the propensity function of each reaction channel, we introduce the basis functions

$$\begin{aligned}\phi_1(x) &= x^{(1)}, & \phi_2(x) &= x^{(2)}, \\ \phi_3(x) &= (x^{(1)})^2, & \phi_4(x) &= x^{(1)}x^{(2)}, & \phi_5(x) &= (x^{(2)})^2.\end{aligned}\tag{46}$$

The propensity functions of the reaction channels are approximated by

$$a_i^{(\epsilon)}(x; \boldsymbol{\omega}) = a_i^{(\epsilon)}(x; \boldsymbol{\omega}^{(i)}) = G_\epsilon \left(\sum_{k=1}^5 \omega_{5(i-1)+k} \phi_k(x) \right), \quad 1 \leq i \leq 4, \tag{47}$$

where G_ϵ is defined in (32) and we set $\epsilon = 0.1$. In (47), the function $a_i^{(\epsilon)}$ depends on the 5 parameters $\boldsymbol{\omega}^{(i)} = (\omega_{5(i-1)+1}, \omega_{5(i-1)+2}, \dots, \omega_{5(i-1)+5})^T$, and the same set of basis functions in (46) is used for each of the 4 channels. See Remark 2 in Subsection 3.3 for related discussions.

To determine the value of $\boldsymbol{\omega} = (\omega_1, \omega_2, \dots, \omega_{20})^T$, which consists of all the unknown parameters, we follow the discussions in Remark 2 of Subsection 3.3 and solve the sparse minimization problems

$$\min_{\boldsymbol{\omega}^{(i)} \in \mathbb{R}^{N_i}} \left\{ -\frac{1}{QT} \sum_{q=1}^Q \left[\sum_{k=1}^{M_i^{(q)}} \ln G_\epsilon \left(\sum_{j \in \mathcal{I}_i} \omega_j \varphi_j(y_{l_k^{(q,i)}}^{(q)}) \right) + \sum_{l=0}^{M^{(q)}} t_l^{(q)} G_\epsilon \left(\sum_{j \in \mathcal{I}_i} \omega_j \varphi_j(y_l^{(q)}) \right) \right] + \lambda \|\boldsymbol{\omega}^{(i)}\|_1 \right\}. \tag{48}$$

For each channel \mathcal{C}_i , (48) is solved separately by applying the “Fast Iterative Shrinkage-Thresholding Algorithm (FISTA) with backtracking” proposed in [7], and $\lambda = 0.1, 0.01, 0.001$ is chosen in this numerical experiment. In each iteration step, evaluating the objective function in (48) as well as its derivative requires traversing every reaction along the 100 trajectories. This part of the calculation is performed in parallel using the numerical package MPI in our code. The iteration procedure continues until the relative difference between the minimal and the maximal values of the objective function in the last 20 iteration steps is smaller than $5 \cdot 10^{-8}$. In this example, we run the code using 20 processors in parallel and it takes only a few seconds to meet the convergence criterion.

The final results are summarized in Table 5. In order to make a comparison with the true parameters in (44), we notice that, with the basis functions in (46), the true propensity functions of the 4 reaction channels in the system (see Table 2) can be expressed as

$$\begin{aligned}a_1^*(x) &= 1.0 x^{(1)} = G_0(1.0 \phi_1(x)), \\ a_2^*(x) &= 0.1 x^{(1)}x^{(2)} = G_0(0.1 \phi_4(x)), \\ a_3^*(x) &= 1.0 x^{(2)} = G_0(1.0 \phi_2(x)), \\ a_4^*(x) &= 0.9 x^{(1)} = G_0(0.9 \phi_1(x)),\end{aligned}\tag{49}$$

where $G_0(x) = \max(x, 0)$. From the above expressions, we can conclude that the propensity functions in (47), with the estimated parameters in Table 5 (for $\lambda = 0.01$ or 0.001), indeed approximate the true propensity functions in (49) quite well.

Table 3: Example 1. The state change vectors v of the 4 reaction channels in the system and the numbers of occurrences of their activations within the 100 trajectories are obtained by analyzing the trajectory data.

Channel	1	2	3	4
Vector v^T	$(-1, 0)$	$(-1, 1)$	$(0, -1)$	$(1, 0)$
No. of occurrence	2296	1778	2777	2135

Table 4: The first learning task in Example 1. The row with label “True” shows the parameters in (44) used to generate the 100 trajectories of the reaction system. The row with label “Estimated” shows the parameters obtained by minimizing the negative log-likelihood function (45).

	κ_1	κ_2	κ_3	κ_4
True	1.0	0.1	1.0	0.9
Estimated	0.98	0.10	0.97	0.91

Table 5: The second learning task in Example 1. The parameters in the propensity functions (47) of the 4 channels are estimated by solving the sparse minimization problems (48), with $\epsilon = 0.1$ and $\lambda = 0.1, 0.01, 0.001$, respectively. For each channel \mathcal{C}_i , $1 \leq i \leq 4$, the same set of basis functions in (46) is used in the estimation. In each row, the estimated parameters $\omega^{(i)} = (\omega_{5(i-1)+1}, \omega_{5(i-1)+2}, \dots, \omega_{5(i-1)+5})^T$, which are involved in (47) in front of the basis functions $x^{(1)}$, $x^{(2)}$, $(x^{(1)})^2$, $x^{(1)}x^{(2)}$, and $(x^{(2)})^2$, are shown. The parameter that has the largest absolute value within the same row is underlined.

Channel	λ	$x^{(1)}$	$x^{(2)}$	$(x^{(1)})^2$	$x^{(1)}x^{(2)}$	$(x^{(2)})^2$
1	0.1	<u>0.80</u>	$-8.3 \cdot 10^{-6}$	$8.4 \cdot 10^{-3}$	$8.3 \cdot 10^{-3}$	$-3.6 \cdot 10^{-4}$
	0.01	<u>0.98</u>	$-5.1 \cdot 10^{-2}$	$-2.3 \cdot 10^{-3}$	$5.4 \cdot 10^{-3}$	$2.2 \cdot 10^{-3}$
	0.001	<u>1.01</u>	$-6.1 \cdot 10^{-2}$	$-4.0 \cdot 10^{-3}$	$5.4 \cdot 10^{-3}$	$2.7 \cdot 10^{-3}$
2	0.1	$-1.7 \cdot 10^{-4}$	$-1.9 \cdot 10^{-2}$	$-1.5 \cdot 10^{-3}$	<u>0.10</u>	0
	0.01	$-2.6 \cdot 10^{-2}$	$-4.4 \cdot 10^{-2}$	$1.6 \cdot 10^{-4}$	<u>0.10</u>	$1.8 \cdot 10^{-3}$
	0.001	$-2.9 \cdot 10^{-2}$	$-4.6 \cdot 10^{-2}$	$4.3 \cdot 10^{-4}$	<u>0.10</u>	$2.0 \cdot 10^{-3}$
3	0.1	0	<u>0.86</u>	$-3.4 \cdot 10^{-3}$	$1.3 \cdot 10^{-3}$	$9.7 \cdot 10^{-3}$
	0.01	$-3.7 \cdot 10^{-2}$	<u>1.02</u>	$-1.8 \cdot 10^{-3}$	$6.4 \cdot 10^{-4}$	$-1.4 \cdot 10^{-3}$
	0.001	$-4.9 \cdot 10^{-2}$	<u>1.05</u>	$-1.2 \cdot 10^{-3}$	$3.9 \cdot 10^{-4}$	$-3.1 \cdot 10^{-3}$
4	0.1	<u>0.75</u>	$-2.0 \cdot 10^{-4}$	$8.1 \cdot 10^{-3}$	$6.0 \cdot 10^{-3}$	0
	0.01	<u>0.93</u>	$-6.7 \cdot 10^{-2}$	$-2.6 \cdot 10^{-3}$	$3.5 \cdot 10^{-3}$	$3.8 \cdot 10^{-3}$
	0.001	<u>0.96</u>	$-7.8 \cdot 10^{-2}$	$-4.2 \cdot 10^{-3}$	$3.4 \cdot 10^{-3}$	$4.4 \cdot 10^{-3}$

4.2 Example 2: predator-prey system

In the second example, we consider the predator-prey type reaction system in Table 6, which has 2 different species and 5 chemical reactions. In contrast to the previous example where different reactions have different state change vectors, in the current case both the reaction $A \xrightarrow{\kappa_2} \emptyset$ and the reaction $A + B \xrightarrow{\kappa_5} B$ have the same state change vector $v = (-1, 0)^T$.

In the first step, we generate the trajectory data of the system with the parameters

$$(\kappa_1, \kappa_2, \kappa_3, \kappa_4, \kappa_5) = (1.2, 0.3, 0.8, 0.75, 0.1). \quad (50)$$

Starting from the state $x = (25, 15)^T$ at time $t = 0$, $Q = 100$ trajectories are simulated using SSA until the terminal time $T = 10$, and 5 of these 100 trajectories are shown in Figure 3 for illustration. After analyzing the trajectory data, we can identify the 4 different reaction channels in the system, as well as the numbers of occurrences of activations for each channel within the 100 trajectories (see Table 7).

Table 6: Example 2. Chemical reaction system of predator-prey type. Two species A and B are involved in 5 chemical reactions. The copy-numbers of the species A, B are denoted by $x = (x^{(1)}, x^{(2)})^T$. Here, κ_i , v , and $a_{\mathcal{R}}^*(x)$ are the rate constant, the state change vector, and the propensity function of the reactions, respectively. The 2nd and the 5th reactions have the same state change vector $v = (-1, 0)^T$ and belong to the same reaction channel \mathcal{C}_1 .

No.	Reaction	v^T	Channel	$a_{\mathcal{R}}^*(x)$
1	$A \xrightarrow{\kappa_1} 2A$	$(1, 0)$	4	$\kappa_1 x^{(1)}$
2	$A \xrightarrow{\kappa_2} \emptyset$	$(-1, 0)$	1	$\kappa_2 x^{(1)}$
3	$B \xrightarrow{\kappa_3} 2B$	$(0, 1)$	3	$\kappa_3 x^{(2)}$
4	$B \xrightarrow{\kappa_4} \emptyset$	$(0, -1)$	2	$\kappa_4 x^{(2)}$
5	$A + B \xrightarrow{\kappa_5} B$	$(-1, 0)$	1	$\kappa_5 x^{(1)} x^{(2)}$

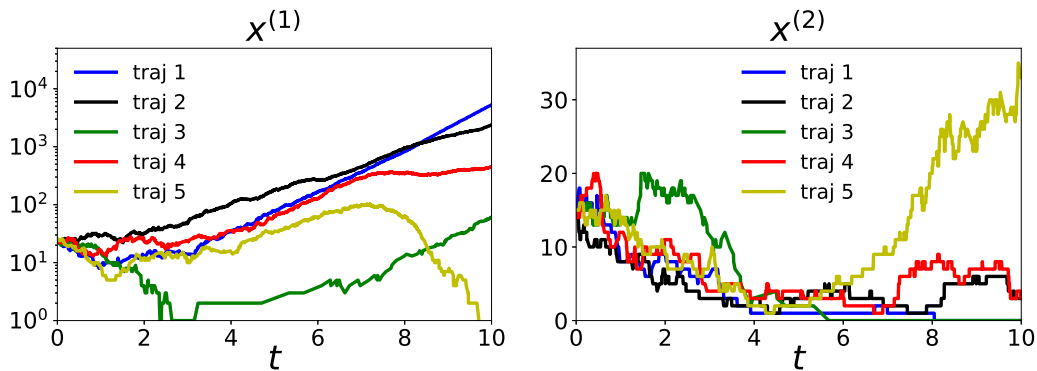


Figure 3: Example 2. The evolution of the system's state $x = (x^{(1)}, x^{(2)})^T$, shown are 5 of the overall 100 trajectories. Note that, unlike the trajectory data in Example 1 (Figure 2), where the copy-numbers of both species A and B stay below 30, in some trajectories of this example the copy-number of the species A ($x^{(1)}$) may grow from 25 to nearly 10^4 within the time interval $[0, 10]$.

Table 7: Example 2. Both the state change vectors v of the 4 reaction channels in the system and the numbers of occurrences of their activations within the 100 trajectories can be obtained by analyzing the trajectory data.

Channel	1	2	3	4
Vector v^T	$(-1, 0)$	$(0, -1)$	$(0, 1)$	$(1, 0)$
No. of occurrence	22828	14065	14840	42837

With the prepared trajectory data, we study the estimation of the parameters κ_i , $1 \leq i \leq 5$, assuming that the structure of the 5 reactions in Table 6 is known (learning task 1). In the same way as we did in the previous example, we consider the minimization of the same negative log-likelihood function (45). The parameters $\kappa_1, \kappa_3, \kappa_4$ can be computed explicitly from the expression which is similar to (27) since the corresponding reaction channel contains only one single reaction, while the parameters κ_2, κ_5 , both of which are involved in the same channel $v^T = (-1, 0)$, can be found using a gradient descent method. In the latter case, we choose the time step-size $\Delta t = 10^{-3}$ and the initial values are set to 1.0. In both cases, it only takes several seconds to run the code and the estimated parameters κ_i are indeed very close to the true parameters (see Table 8).

Table 8: The first learning task in Example 2. The row with label “True” shows the parameters in (50) which are used to generate the 100 trajectories of the system. The row with label “Estimated” shows the parameters obtained by minimizing the negative log-likelihood function (45).

	κ_1	κ_2	κ_3	κ_4	κ_5
True	1.2	0.3	0.8	0.75	0.1
Estimated	1.20	0.30	0.80	0.76	0.10

Next, we study the second learning task described in Subsection 3.3, where our aim is to learn the propensity functions of the 4 identified reaction channels without knowing the structures of the chemical reactions. The propensity functions are approximated in the same way as in (47), with the same set of basis functions in (46) and $\epsilon = 0.1$. For each channel C_i and each $\lambda = 0.1, 0.01, 0.001$, the sparse minimization problem (48) is solved separately by “FISTA with backtracking”, using the same number of processors (i.e., 20) and the same convergence criterion as in the previous example.

However, as shown in Figure 3, the trajectory data in the current example exhibits further complexities, as the copy-number $x^{(1)}$ of the species A in the system varies significantly (from 25 to nearly 10^4) within the time interval $[0, 10]$, unlike the trajectory data in the previous example, where the copy-numbers of the both species stay below 30 (Figure 2). As a result, in Table 9 we see that the different basis functions in (46) are of vastly different orders of magnitude when they are evaluated at the states contained in the 100 trajectories. At the same time, in the numerical experiment we find that direct minimization of (48) using FISTA does not converge at all for any of the 4 reaction channels, due to the extremely small step-size from 10^{-11} to 10^{-8} (the step-size is determined by the method “FISTA with backtracking” itself [7]).

To overcome this difficulty, we apply the idea of preconditioning discussed in Remark 2.

Let φ_j denote the basis functions, where $\varphi_j = \phi_k$, for $j = 5(i - 1) + k$, $1 \leq k \leq 5$. For each index j belonging to the i th channel \mathcal{C}_i , we record the maximal values of φ_j among all the states in the trajectory data at which \mathcal{C}_i has been activated. These maximal values are then used to (empirically) determine the rescaling constants c_j , shown in Table 9 such that the functions φ_j/c_j after rescaling are roughly of the same order of magnitude. As discussed in Remark 2, we solve the rescaled sparse minimization problem, which is similar to (40), for each channel separately, and restore the parameters ω in the propensity functions. It turns out that the problems after rescaling become much easier to solve, because in this case we can increase the step-size to 10^{-5} , which is 3 to 6 orders of magnitude larger than the step-size used in the unrescaled problem. It takes less than 10 minutes in total to meet the convergence criterion for all the 4 reaction channels and the results are summarized in Table 10.

To compare with the true parameters in (50), notice that the true propensity functions of the 4 channels in Table 7 can be expressed as

$$\begin{aligned} a_1^*(x) &= 0.3 x^{(1)} + 0.1 x^{(1)} x^{(2)} = G_0(0.3 \phi_1(x) + 0.1 \phi_4(x)), \\ a_2^*(x) &= 0.75 x^{(2)} = G_0(0.75 \phi_2(x)), \\ a_3^*(x) &= 0.8 x^{(2)} = G_0(0.8 \phi_2(x)), \\ a_4^*(x) &= 1.2 x^{(1)} = G_0(1.2 \phi_1(x)), \end{aligned} \tag{51}$$

where $G_0(x) = \max(x, 0)$. From the expressions above, we can conclude that the propensity functions in (47), together with the parameters given in Table 10 (for $\lambda = 0.01$ or 0.001), indeed approximate the true propensity functions in (51) quite well.

Table 9: Example 2. As discussed in Remark 2, index k , $1 \leq k \leq 5$, counts the different basis functions ϕ_k , while index j , $1 \leq j \leq 20$, counts the basis functions φ_j for all the 4 channels. The same set of basis functions ϕ_k in (46) is used for each of the 4 channels. For each j belonging to channel \mathcal{C}_i , i.e., $5(i - 1) < j \leq 5i$, we have the correspondence $\varphi_j = \phi_k$, if $j = 5(i - 1) + k$. See (39). For each channel \mathcal{C}_i , the column with label “max φ_j ” shows the maximal values of the 5 basis functions ϕ_k (in different rows) evaluated on the trajectory data. The maximal values are computed among all the states in the trajectory data at which \mathcal{C}_i has been activated. The rescaling constants c_j are determined empirically depending on these maximal values, such that the functions φ_j/c_j are roughly of the same order of magnitude.

		Channel 1		Channel 2		Channel 3		Channel 4	
k	ϕ_k	max φ_j	c_j	max φ_j	c_j	max φ_j	c_j	max φ_j	c_j
1	$x^{(1)}$	$5.3 \cdot 10^3$	10	$2.2 \cdot 10^3$	10	$2.1 \cdot 10^3$	10	$5.3 \cdot 10^3$	50
2	$x^{(2)}$	41	1	104	1	103	1	38	1
3	$(x^{(1)})^2$	$2.8 \cdot 10^7$	50000	$4.8 \cdot 10^6$	10000	$4.4 \cdot 10^6$	20000	$2.8 \cdot 10^7$	100000
4	$x^{(1)}x^{(2)}$	$1.1 \cdot 10^4$	100	$1.2 \cdot 10^4$	100	$8.3 \cdot 10^3$	20	$1.2 \cdot 10^4$	100
5	$(x^{(2)})^2$	$1.7 \cdot 10^3$	5	$1.1 \cdot 10^4$	100	$1.1 \cdot 10^4$	50	$1.4 \cdot 10^3$	10

Table 10: The second learning task in Example 2. The parameters in the propensity functions (47) of the 4 channels in Table 7 are estimated, with $\epsilon = 0.1$ and $\lambda = 0.1, 0.01, 0.001$, respectively. As discussed in Remark 2, for each channel i , $1 \leq i \leq 4$, the same set of basis functions in (46) is used and the rescaled version of the sparse minimization problem (48) is solved, by rescaling the basis functions using the constants c_j in Table 9. In each row, the estimated parameters $\omega^{(i)} = (\omega_{5(i-1)+1}, \omega_{5(i-1)+2}, \dots, \omega_{5(i-1)+5})^T$, which are involved in (47) in front of the basis functions $x^{(1)}, x^{(2)}, (x^{(1)})^2, x^{(1)}x^{(2)}$, and $(x^{(2)})^2$, are shown for different λ . The parameters that have relatively significant absolute values within the same row are underlined.

Channel	λ	$x^{(1)}$	$x^{(2)}$	$(x^{(1)})^2$	$x^{(1)}x^{(2)}$	$(x^{(2)})^2$
1	0.1	<u>0.30</u>	$-2.1 \cdot 10^{-2}$	$-6.6 \cdot 10^{-7}$	<u>0.10</u>	$1.7 \cdot 10^{-4}$
	0.01	<u>0.30</u>	$-2.7 \cdot 10^{-2}$	$-1.8 \cdot 10^{-6}$	<u>0.10</u>	$2.7 \cdot 10^{-4}$
	0.001	<u>0.30</u>	$-2.7 \cdot 10^{-2}$	$-2.0 \cdot 10^{-6}$	<u>0.10</u>	$2.7 \cdot 10^{-4}$
2	0.1	$-1.1 \cdot 10^{-3}$	<u>0.73</u>	$2.8 \cdot 10^{-7}$	$3.6 \cdot 10^{-4}$	$8.4 \cdot 10^{-4}$
	0.01	$-1.1 \cdot 10^{-3}$	<u>0.75</u>	$2.8 \cdot 10^{-7}$	$3.1 \cdot 10^{-4}$	$3.9 \cdot 10^{-4}$
	0.001	$-1.0 \cdot 10^{-3}$	<u>0.75</u>	$2.7 \cdot 10^{-7}$	$2.9 \cdot 10^{-4}$	$3.0 \cdot 10^{-4}$
3	0.1	$-3.2 \cdot 10^{-4}$	<u>0.78</u>	$-1.6 \cdot 10^{-7}$	$9.4 \cdot 10^{-5}$	$5.9 \cdot 10^{-4}$
	0.01	$-3.5 \cdot 10^{-4}$	<u>0.80</u>	$-1.0 \cdot 10^{-7}$	$4.9 \cdot 10^{-5}$	$1.5 \cdot 10^{-4}$
	0.001	$-3.7 \cdot 10^{-4}$	<u>0.80</u>	$-9.1 \cdot 10^{-8}$	$4.7 \cdot 10^{-5}$	$1.0 \cdot 10^{-4}$
4	0.1	<u>1.17</u>	$-1.7 \cdot 10^{-2}$	$1.4 \cdot 10^{-5}$	$4.1 \cdot 10^{-3}$	$1.5 \cdot 10^{-4}$
	0.01	<u>1.18</u>	$-2.0 \cdot 10^{-2}$	$1.0 \cdot 10^{-5}$	$3.6 \cdot 10^{-3}$	$2.0 \cdot 10^{-4}$
	0.001	<u>1.18</u>	$-2.0 \cdot 10^{-2}$	$1.0 \cdot 10^{-5}$	$3.6 \cdot 10^{-3}$	$2.1 \cdot 10^{-4}$

4.3 Example 3: reaction network modeling intracellular viral infection

In the third example, we consider the reaction network in [35], which models intracellular viral infection. We refer to [35] for the biological background and to [21, 5] for further studies of this system. As shown in Table 11, the system consists of 4 different species, i.e., the viral template (T), the viral genome (G), the viral structure protein (S), and the virus (V). These species are involved in 6 chemical reactions.

First of all, starting from the state $x = (1, 0, 0, 0)^T$ at time $t = 0$, $Q = 10$ trajectories of the system are generated using SSA until $T = 100$, with the parameters

$$(\kappa_1, \kappa_2, \kappa_3, \kappa_4, \kappa_5, \kappa_6) = (0.25, 0.001, 0.3, 100, 2.0, 0.1) \quad (52)$$

in Table 11. For illustration purposes, 5 of these 10 trajectories are shown in Figure 4. It can be observed that the copy-numbers $x^{(3)}, x^{(4)}$ of S, V may increase to 10^2 – 10^3 , while the copy-numbers $x^{(1)}, x^{(2)}$ of T, G remain relatively small (less than 20) within the time interval $[0, 100]$. After analyzing the trajectory data, we can identify the 6 reaction channels of the system. The numbers of occurrences of activations for each channel within the 10 trajectories can be counted as well (see Table 12).

With these trajectory data, we study the estimation of the parameters κ_i , $1 \leq i \leq 6$, assuming that the structures of the 6 reactions in Table 11 are known (learning task 1). In the same way as we did in the previous two examples, the parameters are estimated by minimizing the same negative log-likelihood function (45). Since each reaction channel contains only one

reaction, the parameters κ_i can be directly computed (see (27)) and are indeed very close to the true parameters in (52), as shown in Table 13.

In what follows, we continue to study the second learning task in Subsection 3.3, where we want to learn the propensity functions of the 6 identified reaction channels in the system without knowing the structures of the chemical reactions. As discussed in Remark 2, since there are 4 different species in the system, we construct the following basis functions

$$\begin{aligned} \phi_1(x) &= x^{(1)}, \quad \phi_2(x) = x^{(2)}, \quad \phi_3(x) = x^{(3)}, \quad \phi_4(x) = x^{(4)}, \\ \phi_5(x) &= (x^{(1)})^2, \quad \phi_6(x) = x^{(1)}x^{(2)}, \quad \phi_7(x) = x^{(1)}x^{(3)}, \quad \phi_8(x) = x^{(1)}x^{(4)}, \\ \phi_9(x) &= (x^{(2)})^2, \quad \phi_{10}(x) = x^{(2)}x^{(3)}, \quad \phi_{11}(x) = x^{(2)}x^{(4)}, \quad \phi_{12}(x) = (x^{(3)})^2, \\ \phi_{13}(x) &= x^{(3)}x^{(4)}, \quad \phi_{14}(x) = (x^{(4)})^2, \end{aligned} \quad (53)$$

where $x = (x^{(1)}, x^{(2)}, x^{(3)}, x^{(4)})^T$, to learn the propensity function of each reaction channel. Similar to (47) in the first example, the propensity functions of the 6 reaction channels are approximated by

$$a_i^{(\epsilon)}(x; \omega) = a_i^{(\epsilon)}(x; \omega^{(i)}) = G_\epsilon \left(\sum_{k=1}^{14} \omega_{14(i-1)+k} \phi_k(x) \right), \quad 1 \leq i \leq 6, \quad (54)$$

with $\epsilon = 0.1$. For each $1 \leq i \leq 6$, the same sparse minimization problem in (48) is solved in order to determine the coefficients $\omega^{(i)} = (\omega_{14(i-1)+1}, \omega_{14(i-1)+2}, \dots, \omega_{14(i-1)+14})^T$. From Table 14, we can again observe that the maximal values of the different basis functions in (53), evaluated for the trajectory data, are of different orders of magnitude. Therefore, the same rescaling strategy discussed in Remark 2 and the previous example is applied to precondition the problem, using the rescaling constants c_j in Table 14 which are determined empirically based on the maximal values of basis functions. Notice that, since for different channels the basis functions attain similar maximal values, the same set of rescaling constants is used for all the 6 channels. For each reaction channel, the rescaled minimization problem is solved in parallel using 10 processors, since the trajectory data only contains 10 trajectories, and the iteration procedure continues until the relative difference between the minimal and the maximal values of the objective function in the last 20 iteration steps is smaller than $1.0 \cdot 10^{-7}$. In total, it takes less than 10 minutes to meet the convergence criterion for all the 6 reaction channels and the estimated coefficients are summarized in Table 15.

To compare with the true propensity functions of the 6 channels in Table 12 with the true parameters in (52), let us write the true propensity functions as

$$\begin{aligned} a_1^*(x) &= 0.25 x^{(1)} = G_0(0.25 \phi_1(x)), \\ a_2^*(x) &= 0.001 x^{(2)}x^{(3)} = G_0(0.001 \phi_{10}(x)), \\ a_3^*(x) &= 0.3 x^{(3)} = G_0(0.3 \phi_3(x)), \\ a_4^*(x) &= 100.0 x^{(1)} = G_0(100.0 \phi_1(x)), \\ a_5^*(x) &= 2.0 x^{(1)} = G_0(2.0 \phi_1(x)), \\ a_6^*(x) &= 0.1 x^{(2)} = G_0(0.1 \phi_2(x)), \end{aligned} \quad (55)$$

where $G_0(x) = \max(x, 0)$. From the expressions above, we can conclude that the propensity functions in (54), together with the estimated parameters in Table 15, indeed approximate the true propensity functions in (55) quite well.

Table 11: Example 3. The reaction network models a type of intracellular viral infection [35]. There are 4 different species in the system, i.e., the viral template (T), the viral genome (G), the viral structure protein (S), and the virus (V), which are involved in 6 chemical reactions. The copy-numbers of T , G , S , and V are denoted by the state vector $x = (x^{(1)}, x^{(2)}, x^{(3)}, x^{(4)})^T$.

No.	Reaction	v^T	Channel	$a_{\mathcal{R}}^*(x)$
1	$T \xrightarrow{\kappa_1} \emptyset$	$(-1, 0, 0, 0)$	1	$\kappa_1 x^{(1)}$
2	$G + S \xrightarrow{\kappa_2} V$	$(0, -1, -1, 1)$	2	$\kappa_2 x^{(2)} x^{(3)}$
3	$S \xrightarrow{\kappa_3} \emptyset$	$(0, 0, -1, 0)$	3	$\kappa_3 x^{(3)}$
4	$T + \text{stuff} \xrightarrow{\kappa_4} T + S$	$(0, 0, 1, 0)$	4	$\kappa_4 x^{(1)}$
5	$T + \text{stuff} \xrightarrow{\kappa_5} T + G$	$(0, 1, 0, 0)$	5	$\kappa_5 x^{(1)}$
6	$G \xrightarrow{\kappa_6} T$	$(1, -1, 0, 0)$	6	$\kappa_6 x^{(2)}$

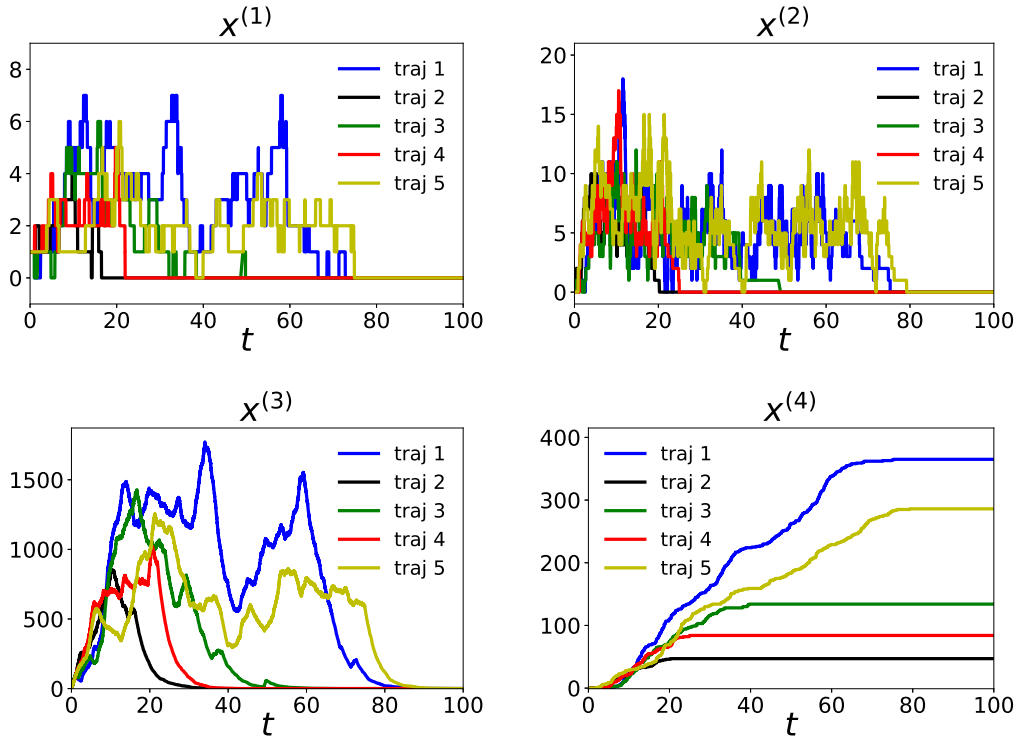


Figure 4: Example 3. The evolution of the system's state $x = (x^{(1)}, x^{(2)}, x^{(3)}, x^{(4)})^T$. Shown are 5 of the overall 10 trajectories. The copy-numbers $x^{(3)}, x^{(4)}$ of S, V can increase to 10^2 – 10^3 , while the copy-numbers $x^{(1)}, x^{(2)}$ of T, G remain relatively small (less than 20) within the time interval $[0, 100]$.

Table 12: Example 3. The state change vectors v of the 6 reaction channels in the system and the numbers of occurrences of their activations within the 10 trajectories can be obtained by analyzing the trajectory data.

Channel	1	2	3	4	5	6
Vector v^T	$(-1, 0, 0, 0)$	$(0, -1, -1, 1)$	$(0, 0, -1, 0)$	$(0, 0, 1, 0)$	$(0, 1, 0, 0)$	$(1, -1, 0, 0)$
No. of occurrence	214	1534	87942	90130	1743	206

Table 13: The first learning task in Example 3. The row with label “True” shows the parameters in (52) which are used to generate the 10 trajectories of the system. The row with label “Estimated” shows the parameters obtained by minimizing the negative log-likelihood function (45).

	κ_1	κ_2	κ_3	κ_4	κ_5	κ_6
True	0.25	0.001	0.3	100.0	2.0	0.1
Estimated	0.24	0.001	0.30	99.3	1.92	0.10

Table 14: Example 3. For the reaction channels $\mathcal{C}_1, \mathcal{C}_2, \dots, \mathcal{C}_6$ in the system, the maximal values of the 14 basis functions ϕ_k in (53) are shown in the columns with label “Ch.1”, “Ch.2”, ..., and “Ch.6”, respectively. The same set of basis functions ϕ_k , $1 \leq k \leq 14$, is used for each of the 6 channels. As discussed in Remark 2, index k counts different basis functions ϕ_k , while index j , $1 \leq j \leq 6 \cdot 14$, counts basis functions φ_j for all the 6 channels. For each j belonging to channel \mathcal{C}_i , i.e., $14(i-1) < j \leq 14i$, we have the correspondence $\varphi_j = \phi_k$, if $j = 14(i-1) + k$. See (39). For each channel \mathcal{C}_i , the column with label “Ch. i ” shows the maximal values of the 14 basis functions ϕ_k (in different rows) evaluated for the trajectory data. The maximal values are computed among all the states in the 10 trajectories at which \mathcal{C}_i has been activated. The rescaling constants c_j are determined empirically, such that after rescaling the basis functions are roughly of the same order of magnitude. Since the basis functions have similar maximal values in different channels, the same rescaling constants are used for all the 6 channels.

k	ϕ_k	$\max \varphi_j$						c_j
		Ch.1	Ch.2	Ch.3	Ch.4	Ch.5	Ch.6	
1	$x^{(1)}$	9	9	9	9	9	8	1
2	$x^{(2)}$	17	18	18	18	17	17	1
3	$x^{(3)}$	1857	1865	1868	1868	1855	1737	10
4	$x^{(4)}$	363	364	365	365	362	362	3
5	$(x^{(1)})^2$	81	81	81	81	81	64	1
6	$x^{(1)}x^{(2)}$	102	119	119	119	112	98	1
7	$x^{(1)}x^{(3)}$	15786	15795	15804	15804	15723	12992	100
8	$x^{(1)}x^{(4)}$	2254	2247	2254	2254	2254	1890	20
9	$(x^{(2)})^2$	289	324	324	324	289	289	2
10	$x^{(2)}x^{(3)}$	20434	26608	26640	26640	24825	20434	200
11	$x^{(2)}x^{(4)}$	2997	3320	3320	3320	2988	3150	30
12	$(x^{(3)})^2$	$3.4 \cdot 10^6$	$3.5 \cdot 10^6$	$3.5 \cdot 10^6$	$3.5 \cdot 10^6$	$3.4 \cdot 10^6$	$3.0 \cdot 10^6$	30000
13	$x^{(3)}x^{(4)}$	514485	515264	516483	516483	514272	509288	5000
14	$(x^{(4)})^2$	131769	132496	133225	133225	131044	131044	1000

Table 15: The second learning task in Example 3. The parameters in the propensity functions (54) of the 6 channels in Table 12 are estimated with $\epsilon = 0.1$. In this example, different λ have been chosen for different reaction channels. For each channel \mathcal{C}_i , $1 \leq i \leq 6$, the rescaled version of the sparse minimization problem (48) is solved by rescaling the basis functions using the constants c_j in Table 14. The same set of basis functions in (53) and the same set of rescaling constants are used in estimating the parameters for all the channels. In each column, the estimated parameters $\omega^{(i)} = (\omega_{14(i-1)+1}, \omega_{14(i-1)+2}, \dots, \omega_{14(i-1)+14})^T$, which are involved in (54) in front of the basis functions ϕ_k are shown. The parameters that have relatively significant absolute values within the same column are underlined.

k	ϕ_k	Ch.1	Ch.2	Ch.3	Ch.4	Ch.5	Ch.6
		$\lambda = 0.01$	$\lambda = 10$	$\lambda = 0.1$	$\lambda = 0.005$	$\lambda = 0.005$	$\lambda = 0.01$
1	$x^{(1)}$	<u>0.28</u>	0	0	<u>94.8</u>	<u>1.86</u>	0
2	$x^{(2)}$	$3.4 \cdot 10^{-3}$	0	0	$-6.9 \cdot 10^{-2}$	$-1.3 \cdot 10^{-2}$	<u>0.11</u>
3	$x^{(3)}$	$-3.6 \cdot 10^{-4}$	0	<u>0.30</u>	$1.3 \cdot 10^{-3}$	$6.7 \cdot 10^{-4}$	$3.5 \cdot 10^{-5}$
4	$x^{(4)}$	$-8.0 \cdot 10^{-4}$	0	$-4.1 \cdot 10^{-4}$	$8.1 \cdot 10^{-4}$	$-2.1 \cdot 10^{-3}$	$-4.5 \cdot 10^{-4}$
5	$(x^{(1)})^2$	0	0	0	$1.3 \cdot 10^{-4}$	$-3.1 \cdot 10^{-2}$	$-2.1 \cdot 10^{-2}$
6	$x^{(1)}x^{(2)}$	$9.4 \cdot 10^{-3}$	0	0	$2.8 \cdot 10^{-1}$	0	$9.4 \cdot 10^{-3}$
7	$x^{(1)}x^{(3)}$	$-1.2 \cdot 10^{-4}$	$4.6 \cdot 10^{-5}$	$-1.8 \cdot 10^{-3}$	$2.4 \cdot 10^{-3}$	$2.6 \cdot 10^{-4}$	$8.8 \cdot 10^{-6}$
8	$x^{(1)}x^{(4)}$	$2.3 \cdot 10^{-4}$	0	$-4.6 \cdot 10^{-4}$	$8.6 \cdot 10^{-3}$	$7.4 \cdot 10^{-4}$	$-2.4 \cdot 10^{-4}$
9	$(x^{(2)})^2$	$-2.7 \cdot 10^{-3}$	0	0	$3.3 \cdot 10^{-3}$	$-2.7 \cdot 10^{-3}$	$-7.0 \cdot 10^{-3}$
10	$x^{(2)}x^{(3)}$	$-2.0 \cdot 10^{-5}$	<u>$9.5 \cdot 10^{-4}$</u>	$6.4 \cdot 10^{-4}$	$1.1 \cdot 10^{-4}$	$1.1 \cdot 10^{-4}$	$8.5 \cdot 10^{-5}$
11	$x^{(2)}x^{(4)}$	$2.5 \cdot 10^{-4}$	$9.5 \cdot 10^{-5}$	$8.1 \cdot 10^{-4}$	$1.5 \cdot 10^{-3}$	$-5.2 \cdot 10^{-4}$	$-1.1 \cdot 10^{-5}$
12	$(x^{(3)})^2$	$6.4 \cdot 10^{-7}$	$-1.7 \cdot 10^{-7}$	$8.2 \cdot 10^{-7}$	$-3.3 \cdot 10^{-6}$	$-1.5 \cdot 10^{-6}$	$-2.0 \cdot 10^{-7}$
13	$x^{(3)}x^{(4)}$	$-1.5 \cdot 10^{-6}$	$6.4 \cdot 10^{-7}$	$3.4 \cdot 10^{-6}$	$-1.2 \cdot 10^{-5}$	$4.6 \cdot 10^{-6}$	$7.7 \cdot 10^{-7}$
14	$(x^{(4)})^2$	$2.1 \cdot 10^{-6}$	$-4.3 \cdot 10^{-7}$	$3.5 \cdot 10^{-7}$	$-4.3 \cdot 10^{-5}$	$-6.4 \cdot 10^{-8}$	$8.5 \cdot 10^{-7}$

5 Asymptotic analysis of the two learning tasks

In this section, we consider the two learning tasks introduced in Section 3 as $T \rightarrow +\infty$. Our main aim is to study the limit behavior of the solutions of the minimization problems (18) and (36). Given the propensity functions a_i^*, a^* of the chemical reaction system in (1), recall that the system's state $X(t)$ satisfies the dynamical equation (3), where \mathcal{P}_i , $1 \leq i \leq K$, are independent unit Poisson processes. In most cases in this section, we will make the following assumptions about the systems. Readers are referred to [32] on the study of ergodicity of stochastic systems.

Assumption 1. *The process $X(t)$ is ergodic and has a unique invariant distribution π on \mathbb{X} .*

Assumption 2. *The basis functions φ_j , $1 \leq j \leq N$, are bounded and nonnegative on \mathbb{X} .*

Our asymptotic analysis approach to study the limit $T \rightarrow +\infty$ crucially relies on the fact that the log-likelihood functions in (19) and (35), as well as their derivatives, can be represented as integrations with respect to the counting processes

$$R_i(t) = \mathcal{P}_i \left(\int_0^t a_i^*(X(s)) ds \right), \quad (56)$$

and the corresponding compensated Poisson processes (martingales)

$$\tilde{R}_i(t) = R_i(t) - \int_0^t a_i^*(X(s)) ds, \quad (57)$$

where $1 \leq i \leq K$ and $t \geq 0$. For instance, it is apparent that the processes R_i are related to M_i in (8), i.e., the number of occurrences of activations for the channel \mathcal{C}_i within the time $[0, T]$, since

$$\begin{aligned} M_i &= R_i(T), \quad 1 \leq i \leq K, \\ \text{and} \quad M &= \sum_{i=1}^K M_i = \sum_{i=1}^K R_i(T). \end{aligned} \quad (58)$$

We refer to Appendix B for two results on the integrations with respect to the processes R_i and \tilde{R}_i , in the $T \rightarrow +\infty$ limit.

5.1 Asymptotic analysis of the log-likelihood maximizer

In this subsection, we consider the first learning task introduced in Subsection 3.2. Recall that $\boldsymbol{\omega}^* = (\omega_1^*, \omega_2^*, \dots, \omega_N^*)^T$ is the true parameter vector such that (15) holds and that

$$a_i^*(x) = a_i(x; \boldsymbol{\omega}^*), \quad \forall x \in \mathbb{X}, \quad 1 \leq i \leq K.$$

For fixed $T > 0$, $\boldsymbol{\omega}^{(T)}$ is the solution of the minimization problem (18). We will study the asymptotic convergence of $\boldsymbol{\omega}^{(T)}$ to $\boldsymbol{\omega}^*$, as $T \rightarrow +\infty$.

Let us first express the log-likelihood function in (19) and its derivatives using the processes in (56) and (57). For the log-likelihood function in (19), since the state of the system is piecewise

constant within $[0, T]$, we obtain

$$\begin{aligned}
& -\ln \mathcal{L}^{(T)}(\boldsymbol{\omega}) \\
&= -\sum_{i=1}^K \int_0^T \left[\ln a_i(X(s); \boldsymbol{\omega}) \right] dR_i + \int_0^T a(X(s); \boldsymbol{\omega}) ds \\
&= -\sum_{i=1}^K \int_0^T \left[\ln a_i(X(s); \boldsymbol{\omega}) \right] d\tilde{R}_i + \sum_{i=1}^K \int_0^T \left[a_i(X(s); \boldsymbol{\omega}) - a_i^*(X(s)) \ln a_i(X(s); \boldsymbol{\omega}) \right] ds,
\end{aligned} \tag{59}$$

while for its first order derivatives in (21), we obtain

$$\begin{aligned}
\mathcal{M}_j^{(T)}(\boldsymbol{\omega}) &= -\int_0^T \frac{\varphi_j(X(s))}{a_i(X(s); \boldsymbol{\omega})} dR_i(s) + \int_0^T \varphi_j(X(s)) ds \\
&= -\int_0^T \frac{\varphi_j(X(s))}{a_i(X(s); \boldsymbol{\omega})} d\tilde{R}_i(s) + \int_0^T \varphi_j(X(s)) \left[1 - \frac{a_i^*(X(s))}{a_i(X(s); \boldsymbol{\omega})} \right] ds,
\end{aligned} \tag{60}$$

for indices j such that $j \in \mathcal{I}_i$. Similarly, for the second order derivatives in (22), we have the expression

$$\begin{aligned}
& \frac{\partial^2 (-\ln \mathcal{L}^{(T)})}{\partial \omega_j \partial \omega_{j'}}(\boldsymbol{\omega}) \\
&= \int_0^T \frac{\varphi_j(X(s)) \varphi_{j'}(X(s))}{a_i^2(X(s); \boldsymbol{\omega})} dR_i(s) \\
&= \int_0^T \frac{\varphi_j(X(s)) \varphi_{j'}(X(s))}{a_i^2(X(s); \boldsymbol{\omega})} d\tilde{R}_i(s) + \int_0^T \frac{\varphi_j(X(s)) \varphi_{j'}(X(s))}{a_i^2(X(s); \boldsymbol{\omega})} a_i^*(X(s)) ds,
\end{aligned} \tag{61}$$

for two indices j, j' such that $j, j' \in \mathcal{I}_i$ for the same i , $1 \leq i \leq K$, and otherwise

$$\frac{\partial^2 (-\ln \mathcal{L}^{(T)})}{\partial \omega_j \partial \omega_{j'}}(\boldsymbol{\omega}) = 0,$$

when $j \in \mathcal{I}_i$ and $j' \in \mathcal{I}_{i'}$ for two different indices $1 \leq i \neq i' \leq K$.

In particular, when $\boldsymbol{\omega} = \boldsymbol{\omega}^*$, the expressions (59) and (60) become simpler and we have

$$\begin{aligned}
-\ln \mathcal{L}^{(T)}(\boldsymbol{\omega}^*) &= -\sum_{i=1}^K \int_0^T \ln a_i^*(X(s)) d\tilde{R}_i + \sum_{i=1}^K \int_0^T a_i^*(X(s)) \left[1 - \ln a_i^*(X(s)) \right] ds, \\
\mathcal{M}_j^{(T)}(\boldsymbol{\omega}^*) &= -\int_0^T \frac{\varphi_j(X(s))}{a_i^*(X(s))} d\tilde{R}_i(s), \quad \forall j \in \mathcal{I}_i.
\end{aligned} \tag{62}$$

5.1.1 Strong consistency

Let us first recall the law of large numbers (LLN) for the unit Poisson processes \mathcal{P}_i , $1 \leq i \leq K$, which states that [1]

$$\lim_{t \rightarrow +\infty} \sup_{u \leq u_0} \left| \frac{\mathcal{P}_i(ut)}{t} - u \right| = 0, \quad a.s., \quad \forall u_0 > 0. \tag{63}$$

It allows us to study the simple case when $N_i = 1$ for a reaction channel \mathcal{C}_i .

Proposition 3. *Given $1 \leq i \leq K$, suppose that $N_i = 1$ and $\mathcal{I}_i = \{j\}$, for some $1 \leq j \leq N$. Assume that*

$$\int_0^T \varphi_j(X(s)) ds \rightarrow +\infty, \quad \text{as } T \rightarrow +\infty, \quad \text{a.s.} \quad (64)$$

Then $\lim_{T \rightarrow +\infty} \omega_j^{(T)} = \omega_j^$, almost surely.*

Proof. As already pointed out in Subsection 3.2, when $N_i = 1$, the Euler–Lagrange equation (21) can be explicitly solved and the solution is given in (27). Using the representations in (56) and (58), we have rewritten (27) as

$$\omega_j^{(T)} = \frac{M_i}{\sum_{l=0}^M t_l \varphi_j(y_l)} = \frac{\mathcal{P}_i\left(\omega_j^* \int_0^T \varphi_j(X(s)) ds\right)}{\int_0^T \varphi_j(X(s)) ds}.$$

Applying the LLN of Poisson processes in (63) together with the assumption (64), we conclude that $\lim_{T \rightarrow +\infty} \omega_j^{(T)} = \omega_j^*$, almost surely. \square

Note that Assumption 1 is not necessary in the above result. In what follows, we continue to study the case $N_i > 1$, i.e., when more than one chemical reactions belong to the i th reaction channel \mathcal{C}_i . We also need the following assumption, which concerns the linear independence of the functions φ_j for each reaction channel \mathcal{C}_i .

Assumption 3. *For each $1 \leq i \leq K$ such that $\mathcal{I}_i = \{j_1, j_2, \dots, j_{N_i}\}$, assuming that the vector $\boldsymbol{\eta} = (\eta_1, \eta_2, \dots, \eta_{N_i})^T \in \mathbb{R}^{N_i}$ satisfies*

$$\sum_{l=1}^{N_i} \eta_l \varphi_{j_l}(x) = 0, \quad \forall x \in \mathbb{X},$$

we obtain $\boldsymbol{\eta} = \mathbf{0}$.

The following lemma guarantees the uniqueness of $\boldsymbol{\omega}^{(T)}$ when T is sufficiently large.

Lemma 1. *Under Assumption 1–3, with probability one, the minimization problem (18)–(19) has a unique solution $\boldsymbol{\omega}^{(T)}$, when T is sufficiently large.*

Proof. Under Assumptions 1 and 3, it is not difficult to see from the expressions (19) and (20) that, with probability one, there is at least one minimizer for large enough T . We show the uniqueness by contradiction. Suppose that, with positive probability, the solution of (18)–(19) is not unique for (an increasing subsequence and therefore) all $T > 0$. According to Proposition 1, we can find an index i , $1 \leq i \leq K$, such that the column vectors $\Phi_{i,l}$ of the matrix Φ_i in (23) are linearly dependent for all $T > 0$. Let us suppose that the states in \mathbb{X} are ordered such that $\mathbb{X} = \{x_1, x_2, \dots\}$ and $m \in \mathbb{N}$ is a positive integer. The ergodicity of the system (Assumption 1) implies that, with probability one, the states x_1, x_2, \dots, x_m will be visited by the system when T is large enough. Since there is positive probability that the vectors $\Phi_{i,l}$ are linearly dependent for all $T > 0$, we can find $\boldsymbol{\eta}^{(m)} \in (\eta_1, \eta_2, \dots, \eta_{N_i})^T \in \mathbb{R}^{N_i}$, such that

$$\sum_{l=1}^{N_i} \eta_l^{(m)} \varphi_{j_l}(x_k) = 0, \quad \forall 1 \leq k \leq m, \quad (65)$$

where $\mathcal{I}_i = \{j_1, j_2, \dots, j_{N_i}\}$. Without loss of generality, we can assume $\|\boldsymbol{\eta}^{(m)}\|_2^2 = 1$ and let $\boldsymbol{\eta}$ be a limit point of the sequence $\boldsymbol{\eta}^{(m)}$ as $m \rightarrow +\infty$. Then (65) implies that

$$\sum_{l=1}^{N_i} \eta_l \varphi_{j_l}(x) = 0, \quad \forall x \in \mathbb{X}.$$

Furthermore, $\boldsymbol{\eta}$ is nonzero since $\|\boldsymbol{\eta}\|_2^2 = \lim_{m \rightarrow +\infty} \|\boldsymbol{\eta}^{(m)}\|_2^2 = 1$. This contradicts Assumption 3. \square

To proceed, we will need the Kullback–Leibler divergence between two probability distributions [30], which is nonnegative and equals zero if and only if the two distributions are identical. In particular, for the probability distributions whose density functions are ψ and p in (4), the Kullback–Leibler divergences can be computed as

$$\begin{aligned} D_{KL}(\psi(\cdot; x, \boldsymbol{\omega}') \mid \psi(\cdot; x, \boldsymbol{\omega})) &= \int_0^{+\infty} \ln \frac{\psi(t; x, \boldsymbol{\omega}')}{\psi(t; x, \boldsymbol{\omega})} \psi(t; x, \boldsymbol{\omega}') dt \\ &= -\ln \frac{a(x; \boldsymbol{\omega})}{a(x; \boldsymbol{\omega}')} + \frac{a(x; \boldsymbol{\omega})}{a(x; \boldsymbol{\omega}')} - 1, \\ D_{KL}(p(\cdot; x, \boldsymbol{\omega}') \mid p(\cdot; x, \boldsymbol{\omega})) &= \sum_{i=1}^K \ln \frac{p(i; x, \boldsymbol{\omega}')}{p(i; x, \boldsymbol{\omega})} p(i; x, \boldsymbol{\omega}') \\ &= \ln \frac{a(x; \boldsymbol{\omega})}{a(x; \boldsymbol{\omega}')} - \sum_{i=1}^K \frac{a_i(x; \boldsymbol{\omega}')}{a(x; \boldsymbol{\omega}')} \ln \frac{a_i(x; \boldsymbol{\omega})}{a_i(x; \boldsymbol{\omega}')}, \end{aligned} \tag{66}$$

respectively, where $x \in \mathbb{X}$ and $\boldsymbol{\omega}, \boldsymbol{\omega}'$ are two parameter vectors in (16).

The convergence of $\boldsymbol{\omega}^{(T)}$ towards $\boldsymbol{\omega}^*$ as $T \rightarrow +\infty$ is established in the following result.

Proposition 4. *Suppose that Assumptions 1–3 hold.*

1. *For any vector $\boldsymbol{\omega}$ in (16), we have*

$$\begin{aligned} &\lim_{T \rightarrow +\infty} \frac{\ln \mathcal{L}^{(T)}(\boldsymbol{\omega}) - \ln \mathcal{L}^{(T)}(\boldsymbol{\omega}^*)}{T} \\ &= \sum_{x \in \mathbb{X}} \left[a(x; \boldsymbol{\omega}^*) - a(x; \boldsymbol{\omega}) + \sum_{i=1}^K \left(a_i(x; \boldsymbol{\omega}^*) \ln \frac{a_i(x; \boldsymbol{\omega})}{a_i(x; \boldsymbol{\omega}^*)} \right) \right] \pi(x) \\ &= - \sum_{x \in \mathbb{X}} \left[D_{KL}(\psi(\cdot; x, \boldsymbol{\omega}^*) \mid \psi(\cdot; x, \boldsymbol{\omega})) + D_{KL}(p(\cdot; x, \boldsymbol{\omega}^*) \mid p(\cdot; x, \boldsymbol{\omega})) \right] a(x; \boldsymbol{\omega}^*) \pi(x) \\ &\leq 0. \end{aligned}$$

2. *Let $\boldsymbol{\omega}^{(T)} = (\omega_1^{(T)}, \omega_2^{(T)}, \dots, \omega_N^{(T)})^T$ be the unique minimizer of the problem (18), such that $\omega_j^{(T)} \geq 0$, for each $1 \leq j \leq N$. With probability one, it holds that*

$$\lim_{T \rightarrow +\infty} \boldsymbol{\omega}^{(T)} = \boldsymbol{\omega}^*. \tag{67}$$

Proof. 1. Under Assumption 1, using the expressions in (59), (62), and applying Lemma 6 in

Appendix B, we can compute

$$\begin{aligned}
& \lim_{T \rightarrow +\infty} \frac{\ln \mathcal{L}^{(T)}(\omega) - \ln \mathcal{L}^{(T)}(\omega^*)}{T} \\
&= \lim_{T \rightarrow +\infty} \left[\frac{1}{T} \sum_{i=1}^K \int_0^T \ln \frac{a_i(X(s); \omega)}{a_i(X(s); \omega^*)} d\tilde{R}_i + \frac{1}{T} \sum_{i=1}^K \int_0^T \left(a_i(X(s); \omega^*) - a_i(X(s); \omega) \right) ds \right. \\
&\quad \left. + \sum_{i=1}^K \int_0^T \left(a_i(X(s); \omega^*) \ln \frac{a_i(X(s); \omega)}{a_i(X(s); \omega^*)} \right) ds \right] \\
&= \sum_{x \in \mathbb{X}} \sum_{i=1}^K \left(a_i(x; \omega^*) - a_i(x; \omega) + a_i(x; \omega^*) \ln \frac{a_i(x; \omega)}{a_i(x; \omega^*)} \right) \pi(x) \\
&= \sum_{x \in \mathbb{X}} \left[a(x; \omega^*) - a(x; \omega) + \sum_{i=1}^K \left(a_i(x; \omega^*) \ln \frac{a_i(x; \omega)}{a_i(x; \omega^*)} \right) \right] \pi(x) \\
&= - \sum_{x \in \mathbb{X}} \left[D_{KL}(\psi(\cdot; x, \omega^*) \mid \psi(\cdot; x, \omega)) + D_{KL}(p(\cdot; x, \omega^*) \mid p(\cdot; x, \omega)) \right] a(x; \omega^*) \pi(x),
\end{aligned} \tag{68}$$

where the last equality follows directly from (66). Therefore, the first conclusion is obtained.

2. Let us first show that the sequence $(\omega_j^{(T)})_{T>0}$ is almost surely bounded for each $1 \leq j \leq N$. From the Euler-Lagrange equation (21), we can obtain the relation

$$\sum_{j \in \mathcal{I}_i} \omega_j^{(T)} \left(\sum_{l=0}^M t_l \varphi_j(y_l) \right) = M_i, \quad \forall 1 \leq i \leq K,$$

which clearly implies that

$$0 \leq \omega_j^{(T)} \leq \frac{M_i}{\sum_{l=0}^M t_l \varphi_j(y_l)} = \frac{\frac{1}{T} \int_0^T 1 dR_i(s)}{\frac{1}{T} \int_0^T \varphi_j(X(s)) ds}, \tag{69}$$

where i , $1 \leq i \leq K$, is the index such that $j \in \mathcal{I}_i$. Notice that both the numerator and the denominator on the right hand side of (69) converge, as consequences of Lemma 6 in Appendix B and the ergodicity of the system (Assumption 1), respectively. Taking the limit $T \rightarrow +\infty$ in (69) and using (17), we have

$$\limsup_{T \rightarrow +\infty} \omega_j^{(T)} \leq \lim_{T \rightarrow +\infty} \frac{\frac{1}{T} \int_0^T 1 dR_i(s)}{\frac{1}{T} \int_0^T \varphi_j(X(s)) ds} = \frac{\sum_{x \in \mathbb{X}} \left[\sum_{j' \in \mathcal{I}_i} \omega_{j'}^* \varphi_{j'}(x) \right] \pi(x)}{\sum_{x \in \mathbb{X}} \varphi_j(x) \pi(x)}, \quad a.s.,$$

which implies that the sequence $(\omega_j^{(T)})_{T>0}$ is almost surely bounded.

From (60), we know that the minimizer $\omega^{(T)}$ satisfies the identity

$$\int_0^T \frac{\varphi_j(X(s))}{a_i(X(s); \omega^{(T)})} dR_i(s) = \int_0^T \varphi_j(X(s)) ds.$$

In particular, for each $x \in \mathbb{X}$, it implies

$$\frac{\varphi_j(x)}{a_i(x; \boldsymbol{\omega}^{(T)})} \int_0^T \mathbf{1}_x(X(s)) dR_i(s) = \int_0^T \frac{\varphi_j(X(s)) \mathbf{1}_x(X(s))}{a_i(X(s); \boldsymbol{\omega}^{(T)})} dR_i(s) \leq \int_0^T \varphi_j(X(s)) ds,$$

where $\mathbf{1}_x$ denotes the indicator function at the state x . Therefore, applying Lemma 6 in Appendix B and using the ergodicity of the system, we have

$$\liminf_{T \rightarrow +\infty} a_i(x; \boldsymbol{\omega}^{(T)}) \geq \varphi_j(x) \lim_{T \rightarrow +\infty} \frac{\int_0^T \mathbf{1}_x(X(s)) dR_i(s)}{\int_0^T \varphi_j(X(s)) ds} = \frac{\varphi_j(x) \pi(x)}{\sum_{x' \in \mathbb{X}} \varphi_j(x') \pi(x')} a_i(x; \boldsymbol{\omega}^*), \quad (70)$$

for all $x \in \mathbb{X}$.

Now let $\bar{\boldsymbol{\omega}}$ be a limit point of $\boldsymbol{\omega}^{(T)}$ as $T \rightarrow +\infty$. Using a similar derivation as in (68) and taking the lower bound (70) into account, we can obtain

$$\begin{aligned} & \lim_{T \rightarrow +\infty} \frac{\ln \mathcal{L}^{(T)}(\boldsymbol{\omega}^{(T)}) - \ln \mathcal{L}^{(T)}(\boldsymbol{\omega}^*)}{T} \\ &= - \sum_{x \in \mathbb{X}} \left[D_{KL}(\psi(\cdot; x, \boldsymbol{\omega}^*) \mid \psi(\cdot; x, \bar{\boldsymbol{\omega}})) + D_{KL}(p(\cdot; x, \boldsymbol{\omega}^*) \mid p(\cdot; x, \bar{\boldsymbol{\omega}})) \right] a_i(x; \boldsymbol{\omega}^*) \pi(x) \\ &\leq 0. \end{aligned} \quad (71)$$

On the other hand, since $\boldsymbol{\omega}^{(T)}$ is the minimizer of the minimization problem (18), we also have that

$$\lim_{T \rightarrow +\infty} \frac{\ln \mathcal{L}^{(T)}(\boldsymbol{\omega}^{(T)}) - \ln \mathcal{L}^{(T)}(\boldsymbol{\omega}^*)}{T} \geq 0.$$

Therefore, the Kullback–Leibler divergences in (71) must be zero at each state x . From the expressions in (66), we get

$$a_i(x; \bar{\boldsymbol{\omega}}) = a_i(x; \boldsymbol{\omega}^*), \quad \forall 1 \leq i \leq K, \quad x \in \mathbb{X}.$$

Using the expression (17) and Assumption 3, we conclude that $\bar{\boldsymbol{\omega}} = \boldsymbol{\omega}^*$ and the convergence (67) is obtained. \square

5.1.2 Asymptotic normality

We now study the asymptotic normality of the sequence $\boldsymbol{\omega}^{(T)}$ as $T \rightarrow +\infty$.

Proposition 5. *Suppose that Assumptions 1–3 hold. Let \mathcal{F} be the $N \times N$ matrix whose entries are given by*

$$\mathcal{F}_{j,j'} = \begin{cases} \sum_{x \in \mathbb{X}} \frac{\varphi_j(x) \varphi_{j'}(x)}{a_i(x; \boldsymbol{\omega}^*)} \pi(x), & \text{if } j, j' \in \mathcal{I}_i, \text{ for some } 1 \leq i \leq K, \\ 0, & \text{otherwise,} \end{cases} \quad (72)$$

for $1 \leq j, j' \leq N$. Then, as $T \rightarrow +\infty$, $\sqrt{T}(\boldsymbol{\omega}^{(T)} - \boldsymbol{\omega}^*)$ converges in distribution to $\mathcal{Z} \sim \mathcal{N}(\mathbf{0}, \mathcal{F}^{-1})$, i.e., \mathcal{Z} is a Gaussian random variable whose mean is zero and whose variance matrix is \mathcal{F}^{-1} .

Proof. First of all, under Assumption 3, it is straightforward to verify that \mathcal{F} is positive definite and therefore invertible. Given $1 \leq j \leq N$, expanding the function $\mathcal{M}_j^{(T)}(\omega)$ in (21) and using (22), we have

$$\mathcal{M}_j^{(T)}(\omega^{(T)}) - \mathcal{M}_j^{(T)}(\omega^*) = \sum_{j'=1}^N \left[\int_0^1 \frac{\partial \mathcal{M}_j^{(T)}}{\partial \omega_{j'}} (\theta \omega^{(T)} + (1-\theta) \omega^*) d\theta \right] (\omega_{j'}^{(T)} - \omega_{j'}^*). \quad (73)$$

Since $\mathcal{M}_j^{(T)}(\omega^{(T)}) = 0$, dividing both sides of the above equality by \sqrt{T} , using (61) and (62), we have

$$\frac{1}{\sqrt{T}} \int_0^T \frac{\varphi_j(X(s))}{a_i(X(s); \omega^*)} d\tilde{R}_i(s) = \sum_{j'=1}^N \mathcal{B}_{j,j'}^{(T)} \left[\sqrt{T} (\omega_{j'}^{(T)} - \omega_{j'}^*) \right], \quad (74)$$

where the index i satisfies $j \in \mathcal{I}_i$, $1 \leq i \leq K$, and we have introduced

$$\begin{aligned} \mathcal{B}_{j,j'}^{(T)} &= \frac{1}{T} \int_0^1 \frac{\partial \mathcal{M}_j^{(T)}}{\partial \omega_{j'}} (\theta \omega^{(T)} + (1-\theta) \omega^*) d\theta \\ &= \frac{1}{T} \int_0^T \left[\int_0^1 \frac{\varphi_j(X(s)) \varphi_{j'}(X(s))}{[a_i(X(s); \theta \omega^{(T)} + (1-\theta) \omega^*)]^2} d\theta \right] dR_i(s), \end{aligned}$$

if $j, j' \in \mathcal{I}_i$, for some $1 \leq i \leq K$, and $\mathcal{B}_{j,j'}^{(T)} = 0$, otherwise.

Let $\mathcal{B}^{(T)}$ denote the $N \times N$ matrix whose entries are $\mathcal{B}_{j,j'}^{(T)}$, and by $\mathcal{W}^{(T)}$ the N -dimensional vector whose component $\mathcal{W}_j^{(T)}$ equals the left-hand side of (74). With this notation, (74) can be written as

$$\mathcal{W}^{(T)} = \mathcal{B}^{(T)} \left[\sqrt{T} (\omega^{(T)} - \omega^*) \right]. \quad (75)$$

Applying Lemma 7 in Appendix B, we know that as $T \rightarrow +\infty$ the vector $\mathcal{W}^{(T)}$ converges in distribution to a Gaussian random variable whose mean equals zero and whose variance matrix is given by \mathcal{F} . Since $\lim_{T \rightarrow +\infty} \omega^{(T)} = \omega^*$ almost surely according to Proposition 4, Lemma 6 in Appendix B implies

$$\lim_{T \rightarrow +\infty} \mathcal{B}^{(T)} = \mathcal{F}, \quad a.s.$$

Therefore, applying Slutsky's Theorem [16], we can conclude

$$\sqrt{T} (\omega^{(T)} - \omega^*) = (\mathcal{B}^{(T)})^{-1} \mathcal{W}^{(T)} \implies \mathcal{Z} \in \mathcal{N}(0, \mathcal{F}^{-1}),$$

as $T \rightarrow +\infty$. □

5.2 Asymptotic analysis of the sparse optimization problem

Based on the analysis in Subsection 5.1, in this subsection we study the minimizer $\omega^{(T, \epsilon, \lambda)}$ of the sparse minimization problem (36) as $T \rightarrow +\infty$, where both $\epsilon = \epsilon(T)$ and $\lambda = \lambda(T)$ depend on T .

Recall the basis functions φ_j in (28) and the index set \mathcal{I}_i in (29). Similar to (60) and (61), let us first express the derivatives of the log-likelihood function in (35) using the processes in

(56) and (57). For the first order derivative (42), we have

$$\begin{aligned}
& \mathcal{M}_j^{(T,\epsilon)}(\boldsymbol{\omega}) \\
&= - \int_0^T (\ln G_\epsilon)' \left(\sum_{j' \in \mathcal{I}_i} \omega_{j'} \varphi_{j'}(X(s)) \right) \varphi_j(X(s)) dR_i(s) + \int_0^T G'_\epsilon \left(\sum_{j' \in \mathcal{I}_i} \omega_{j'} \varphi_{j'}(X(s)) \right) \varphi_j(X(s)) ds \\
&= - \int_0^T (\ln G_\epsilon)' \left(\sum_{j' \in \mathcal{I}_i} \omega_{j'} \varphi_{j'}(X(s)) \right) \varphi_j(X(s)) d\tilde{R}_i(s) \\
&\quad + \int_0^T G'_\epsilon \left(\sum_{j' \in \mathcal{I}_i} \omega_{j'} \varphi_{j'}(X(s)) \right) \varphi_j(X(s)) \left(1 - \frac{a_i^*(X(s))}{G_\epsilon \left(\sum_{j' \in \mathcal{I}_i} \omega_{j'} \varphi_{j'}(X(s)) \right)} \right) ds,
\end{aligned}$$

and for the second order derivatives, we have

$$\begin{aligned}
& \frac{\partial^2 (-\ln \mathcal{L}^{(T,\epsilon)})}{\partial \omega_j \partial \omega_{j'}}(\boldsymbol{\omega}) \\
&= - \int_0^T (\ln G_\epsilon)'' \left(\sum_{k \in \mathcal{I}_i} \omega_k \varphi_k(X(s)) \right) \varphi_j(X(s)) \varphi_{j'}(X(s)) dR_i(s) \\
&\quad + \int_0^T G''_\epsilon \left(\sum_{k \in \mathcal{I}_i} \omega_k \varphi_k(X(s)) \right) \varphi_j(X(s)) \varphi_{j'}(X(s)) ds \\
&= - \int_0^T (\ln G_\epsilon)'' \left(\sum_{k \in \mathcal{I}_i} \omega_k \varphi_k(X(s)) \right) \varphi_j(X(s)) \varphi_{j'}(X(s)) d\tilde{R}_i(s) \\
&\quad + \int_0^T \varphi_j(X(s)) \varphi_{j'}(X(s)) \left[G''_\epsilon \left(\sum_{k \in \mathcal{I}_i} \omega_k \varphi_k(X(s)) \right) - (\ln G_\epsilon)'' \left(\sum_{k \in \mathcal{I}_i} \omega_k \varphi_k(X(s)) \right) a_i^*(X(s)) \right] ds
\end{aligned}$$

when there is an index i , $1 \leq i \leq K$, such that $j, j' \in \mathcal{I}_i$, and otherwise

$$\frac{\partial^2 (-\ln \mathcal{L}^{(T,\epsilon)})}{\partial \omega_j \partial \omega_{j'}}(\boldsymbol{\omega}) = 0,$$

when $j \in \mathcal{I}_i$, $j' \in \mathcal{I}_{i'}$, for two different indices $1 \leq i \neq i' \leq K$.

Since in the current case the components of $\boldsymbol{\omega}^{(T,\epsilon,\lambda)}$ can be negative in principle, we need the following assumption in order to guarantee the boundedness of $\boldsymbol{\omega}^{(T,\epsilon,\lambda)}$, $T > 0$.

Assumption 4. For each $1 \leq i \leq K$, assume that the index set $\mathcal{I}_i = \{j_1, j_2, \dots, j_{N_i}\}$ and the sequence of vectors $\boldsymbol{\eta}^{(k)} = (\eta_1^{(k)}, \eta_2^{(k)}, \dots, \eta_{N_i}^{(k)})^T$, $k \geq 1$, satisfies $\lim_{k \rightarrow +\infty} \|\boldsymbol{\eta}^{(k)}\|_2 = +\infty$. Then $\exists x \in \mathbb{X}$, such that $a_i^*(x) > 0$ and

$$\lim_{k \rightarrow +\infty} \left| \sum_{l=1}^{N_i} \eta_l^{(k)} \varphi_{j_l}(x) \right| = +\infty.$$

Remark 3. Say something about when the above assumption holds.

Lemma 2. Suppose that Assumptions 1 and 2 hold. The parameter $\epsilon = \epsilon(T)$ satisfies $\lim_{T \rightarrow +\infty} \epsilon(T) = 0$. Let $\boldsymbol{\omega}^{(T,\epsilon,\lambda)}$ be the minimizer of the minimization problem (36) and $\mathcal{L}^{(T,\epsilon)}$ be the likelihood function in (35). Assume that

$$\limsup_{T \rightarrow +\infty} -\frac{1}{T} \ln \mathcal{L}^{(T,\epsilon)}(\boldsymbol{\omega}^{(T,\epsilon,\lambda)}) < +\infty, \quad a.s. \quad (76)$$

Then, for each index i , $1 \leq i \leq K$, and $x \in \mathbb{X}$, such that $a_i^*(x) > 0$, we have

$$0 < \liminf_{T \rightarrow +\infty} \left(\sum_{j' \in \mathcal{I}_i} \omega_{j'}^{(T, \epsilon, \lambda)} \varphi_{j'}(x) \right) \leq \limsup_{T \rightarrow +\infty} \left(\sum_{j' \in \mathcal{I}_i} \omega_{j'}^{(T, \epsilon, \lambda)} \varphi_{j'}(x) \right) < +\infty, \quad a.s. \quad (77)$$

Assuming furthermore Assumption 4 holds, then the sequence $\omega^{(T, \epsilon, \lambda)}$, $T > 0$, is bounded.

Proof. We prove (77) by contradiction. Suppose it does not hold, applying Lemma 4 in Appendix A, we can find an index i , $1 \leq i \leq K$ and a state $x \in \mathbb{X}$, satisfying $a_i^*(x) > 0$, such that by extracting a subsequence, which will be again denoted by $\omega^{(T, \epsilon, \lambda)}$, we have either

$$\begin{aligned} & \lim_{T \rightarrow +\infty} G_\epsilon \left(\sum_{j' \in \mathcal{I}_i} \omega_{j'}^{(T, \epsilon, \lambda)} \varphi_{j'}(x) \right) = 0, \\ \text{or} \quad & \lim_{T \rightarrow +\infty} G_\epsilon \left(\sum_{j' \in \mathcal{I}_i} \omega_{j'}^{(T, \epsilon, \lambda)} \varphi_{j'}(x) \right) = +\infty. \end{aligned} \quad (78)$$

Using (35), we can estimate

$$\begin{aligned} & -\frac{1}{T} \ln \mathcal{L}^{(T, \epsilon)}(\omega^{(T, \epsilon, \lambda)}) \\ &= \sum_{i'=1}^K \left[-\frac{1}{T} \int_0^T \ln G_\epsilon \left(\sum_{j \in \mathcal{I}_{i'}} \omega_j^{(T, \epsilon, \lambda)} \varphi_j(X(s)) \right) dR_{i'}(s) + \frac{1}{T} \int_0^T G_\epsilon \left(\sum_{j \in \mathcal{I}_{i'}} \omega_j^{(T, \epsilon, \lambda)} \varphi_j(X(s)) \right) ds \right] \\ &= \sum_{i'=1}^K \sum_{x' \in \mathbb{X}} \left[-\ln G_\epsilon \left(\sum_{j \in \mathcal{I}_{i'}} \omega_j^{(T, \epsilon, \lambda)} \varphi_j(x') \right) \frac{1}{T} \int_0^T \mathbf{1}_{x'}(X(s)) dR_{i'}(s) \right. \\ & \quad \left. + G_\epsilon \left(\sum_{j \in \mathcal{I}_{i'}} \omega_j^{(T, \epsilon, \lambda)} \varphi_j(x') \right) \frac{1}{T} \int_0^T \mathbf{1}_{x'}(X(s)) ds \right] \\ &\geq \sum_{x' \neq x} \sum_{i'=1}^K \left[-\left(\frac{1}{T} \int_0^T \mathbf{1}_{x'}(X(s)) dR_{i'}(s) \right) \ln \frac{\frac{1}{T} \int_0^T \mathbf{1}_{x'}(X(s)) dR_{i'}(s)}{\frac{1}{T} \int_0^T \mathbf{1}_{x'}(X(s)) ds} + \frac{1}{T} \int_0^T \mathbf{1}_{x'}(X(s)) dR_{i'}(s) \right] \\ & \quad + \sum_{1 \leq i' \leq K, i' \neq i} \left[-\left(\frac{1}{T} \int_0^T \mathbf{1}_x(X(s)) dR_{i'}(s) \right) \ln \frac{\frac{1}{T} \int_0^T \mathbf{1}_x(X(s)) dR_{i'}(s)}{\frac{1}{T} \int_0^T \mathbf{1}_x(X(s)) ds} + \frac{1}{T} \int_0^T \mathbf{1}_x(X(s)) dR_{i'}(s) \right] \\ & \quad + \left[-\ln G_\epsilon \left(\sum_{j \in \mathcal{I}_i} \omega_j^{(T, \epsilon, \lambda)} \varphi_j(x) \right) \frac{1}{T} \int_0^T \mathbf{1}_x(X(s)) dR_i(s) + G_\epsilon \left(\sum_{j \in \mathcal{I}_i} \omega_j^{(T, \epsilon, \lambda)} \varphi_j(x) \right) \frac{1}{T} \int_0^T \mathbf{1}_x(X(s)) ds \right] \\ &=: J_1 + J_2 + J_3. \end{aligned} \quad (79)$$

where we have used Lemma 3 below, as well as the convention $0 \ln 0 = 0$. Since $a_i^*(x) > 0$, applying Lemma 6 in Appendix B, we have

$$\lim_{T \rightarrow +\infty} \frac{1}{T} \int_0^T \mathbf{1}_x(X(s)) dR_i = a_i^*(x) \pi(x) > 0, \quad a.s.$$

Therefore, Lemma 3 below implies that we have

$$\lim_{T \rightarrow +\infty} J_3 = +\infty, \quad a.s.$$

in the both cases in (78). For the same reason, applying Lemma 6 in Appendix B, we know that

$$\begin{aligned} \lim_{T \rightarrow +\infty} J_1 &= \sum_{x' \neq x} \pi(x') \sum_{i'=1}^K \left(-a_{i'}^*(x') \ln a_{i'}^*(x') + a_{i'}^*(x') \right) > -\infty, \\ \lim_{T \rightarrow +\infty} J_2 &= \pi(x) \sum_{1 \leq i' \leq K, i' \neq i} \left(-a_{i'}^*(x) \ln a_{i'}^*(x) + a_{i'}^*(x) \right) > -\infty. \end{aligned}$$

Taking the limit $T \rightarrow +\infty$ in (79), we obtain

$$\limsup_{T \rightarrow +\infty} -\frac{1}{T} \ln \mathcal{L}^{(T, \epsilon)}(\boldsymbol{\omega}^{(T, \epsilon, \lambda)}) = +\infty,$$

which contradicts the assumption in (76) and, as a result, (77) has been proved. The boundedness of the sequence $\boldsymbol{\omega}^{(T, \epsilon, \lambda)}$ follows directly from (77) and the Assumption 4. \square

The following elementary lemma has been used in the above proof.

Lemma 3. *Consider the function $f(x) = -c_1 \ln x + c_2 x$, where $c_1 \geq 0, c_2 > 0$ are two constants. We have*

1. $f(x)$ is convex on $(0, +\infty)$.
2. $f(x) \geq -c_1 \ln \frac{c_1}{c_2} + c_1, \forall x \in (0, +\infty)$, and $\lim_{x \rightarrow +\infty} f(x) = +\infty$.
3. When $c_1 > 0$, then $\lim_{x \rightarrow 0+} f(x) = +\infty$.

Recall that ψ^*, p^* are the probability distribution (density) in (2). With the convention $G_0(x) = \lim_{\epsilon \rightarrow 0+} G_\epsilon(x) = \max(x, 0)$, we will denote

$$a_i^{(0)}(x; \boldsymbol{\omega}) = \max\left(\sum_{j \in \mathcal{I}_i} \omega_j \varphi_j(x), 0\right), \quad a^{(0)}(x; \boldsymbol{\omega}) = \sum_{i=1}^K \max\left(\sum_{j \in \mathcal{I}_i} \omega_j \varphi_j(x), 0\right)$$

and, correspondingly,

$$\begin{aligned} \psi^{(0)}(t; x, \boldsymbol{\omega}) &= a^{(0)}(x; \boldsymbol{\omega}) \exp(-a^{(0)}(x; \boldsymbol{\omega})t), \quad t \geq 0, \\ p^{(0)}(i; x, \boldsymbol{\omega}) &= \frac{a_i^{(0)}(x; \boldsymbol{\omega})}{a^{(0)}(x; \boldsymbol{\omega})}, \quad 1 \leq i \leq K. \end{aligned}$$

Now we are ready to state the asymptotic results for the sequence $(\boldsymbol{\omega}^{(T, \epsilon, \lambda)})_{T>0}$, as $T \rightarrow +\infty$. Since the arguments are similar to those used in Proposition 4 and Proposition 5, we will present the proofs of the following results briefly.

Proposition 6. *Suppose that Assumption 1, 2, and 4 are satisfied. The parameters $\lambda = \lambda(T)$, $\epsilon = \epsilon(T)$ in the minimization problem (36) satisfy*

$$\lim_{T \rightarrow +\infty} \lambda(T) = 0, \quad \lim_{T \rightarrow +\infty} \epsilon(T) = 0, \quad (80)$$

and the minimizer $\boldsymbol{\omega}^{(T, \epsilon, \lambda)}$ of (36) satisfies

$$\limsup_{T \rightarrow +\infty} -\frac{1}{T} \ln \mathcal{L}^{(T, \epsilon)}(\boldsymbol{\omega}^{(T, \epsilon, \lambda)}) < +\infty, \quad a.s.$$

Let $\bar{\boldsymbol{\omega}}$ be a limit point of $\boldsymbol{\omega}^{(T, \epsilon, \lambda)}$ as $T \rightarrow +\infty$. For all $\boldsymbol{\omega} \in \mathbb{R}^N$, we have

$$\begin{aligned} & \sum_{x \in \mathbb{X}} \left[D_{KL}(\psi^*(\cdot; x) \mid \psi^{(0)}(\cdot; x, \bar{\boldsymbol{\omega}})) + D_{KL}(p^*(\cdot; x) \mid p^{(0)}(\cdot; x, \bar{\boldsymbol{\omega}})) \right] a^*(x) \pi(x) \\ & \leq \sum_{x \in \mathbb{X}} \left[D_{KL}(\psi^*(\cdot; x) \mid \psi^{(0)}(\cdot; x, \boldsymbol{\omega})) + D_{KL}(p^*(\cdot; x) \mid p^{(0)}(\cdot; x, \boldsymbol{\omega})) \right] a^*(x) \pi(x). \end{aligned} \quad (81)$$

In particular, if there is a unique vector $\boldsymbol{\omega}^* \in \mathbb{R}^N$, such that

$$a_i^*(x) = a_i^{(0)}(x; \boldsymbol{\omega}^*), \quad \forall x \in \mathbb{X}, \quad 1 \leq i \leq K. \quad (82)$$

then

$$\lim_{T \rightarrow +\infty} \boldsymbol{\omega}^{(T, \epsilon, \lambda)} = \boldsymbol{\omega}^*, \quad a.s. \quad (83)$$

Proof. Lemma 2 implies that the sequence $\boldsymbol{\omega}^{(T, \epsilon, \lambda)}$, $T > 0$, is bounded. Similar to (35), let us define

$$-\ln \mathcal{L}^{(T),*} = - \sum_{l=0}^{M-1} \ln a_{i_l}^*(y_l) + \sum_{l=0}^M t_l a^*(y_l).$$

Using a similar derivation as in (68), we can obtain

$$\begin{aligned} & \lim_{T \rightarrow +\infty} \frac{\ln \mathcal{L}^{(T, \epsilon)}(\boldsymbol{\omega}^{(T, \epsilon, \lambda)}) - \ln \mathcal{L}^{(T),*}}{T} \\ &= - \sum_{x \in \mathbb{X}} \left[D_{KL}(\psi^*(\cdot; x) \mid \psi^{(0)}(\cdot; x, \bar{\boldsymbol{\omega}})) + D_{KL}(p^*(\cdot; x) \mid p^{(0)}(\cdot; x, \bar{\boldsymbol{\omega}})) \right] a^*(x) \pi(x), \end{aligned} \quad (84)$$

and

$$\begin{aligned} & \lim_{T \rightarrow +\infty} \frac{\ln \mathcal{L}^{(T, \epsilon)}(\boldsymbol{\omega}) - \ln \mathcal{L}^{(T),*}}{T} \\ &= - \sum_{x \in \mathbb{X}} \left[D_{KL}(\psi^*(\cdot; x) \mid \psi^{(0)}(\cdot; x, \boldsymbol{\omega})) + D_{KL}(p^*(\cdot; x) \mid p^{(0)}(\cdot; x, \boldsymbol{\omega})) \right] a^*(x) \pi(x). \end{aligned} \quad (85)$$

Since $\boldsymbol{\omega}^{(T, \epsilon, \lambda)}$ is the minimizer of the problem (36), we have

$$\begin{aligned} & \frac{1}{T} \left(-\ln \mathcal{L}^{(T, \epsilon)}(\boldsymbol{\omega}^{(T, \epsilon, \lambda)}) + \ln \mathcal{L}^{(T),*} \right) + \lambda(T) \|\boldsymbol{\omega}^{(T, \epsilon, \lambda)}\|_1 \\ & \leq \frac{1}{T} \left(-\ln \mathcal{L}^{(T, \epsilon)}(\boldsymbol{\omega}) + \ln \mathcal{L}^{(T),*} \right) + \lambda(T) \|\boldsymbol{\omega}\|_1. \end{aligned}$$

(81) follows by taking the limit $T \rightarrow +\infty$ in the above inequality, and using (80), (84), and (85).

In particular, when (82) holds, taking $\boldsymbol{\omega} = \boldsymbol{\omega}^*$ in (81), we get

$$\sum_{x \in \mathbb{X}} \left[D_{KL}(\psi^{(0)}(\cdot; x, \boldsymbol{\omega}^*) \mid \psi^{(0)}(\cdot; x, \bar{\boldsymbol{\omega}})) + D_{KL}(p^{(0)}(\cdot; x, \boldsymbol{\omega}^*) \mid p^{(0)}(\cdot; x, \bar{\boldsymbol{\omega}})) \right] a^*(x) \pi(x) = 0,$$

which implies

$$a_i^{(0)}(x; \bar{\boldsymbol{\omega}}) = a_i^{(0)}(x; \boldsymbol{\omega}^*), \quad \forall 1 \leq i \leq K, \quad x \in \mathbb{X}.$$

From the uniqueness of $\boldsymbol{\omega}^*$, we can conclude $\bar{\boldsymbol{\omega}} = \boldsymbol{\omega}^*$ and therefore the convergence (83) is obtained. \square

Proposition 7. Suppose that Assumption 1, 2, and 4 are satisfied. Let \mathcal{F} be the $N \times N$ matrix whose entries are given in (72) and $\boldsymbol{\omega}^{(T, \epsilon, \lambda)}$ be the minimizer of the problem (36). Further assume that the following conditions are met.

1. There is a unique vector $\boldsymbol{\omega}^* \in \mathbb{R}^N$, such that

$$a_i^*(x) = a_i^{(0)}(x; \boldsymbol{\omega}^*), \quad \forall x \in \mathbb{X}, \quad 1 \leq i \leq K,$$

and

$$\inf_{x \in \mathbb{X}} \left| \sum_{j \in \mathcal{I}_i} \omega_j^* \varphi_j(x) \right| = c > 0, \quad \forall 1 \leq i \leq K.$$

2. The parameters $\lambda = \lambda(T)$, $\epsilon = \epsilon(T)$ in (36) satisfy

$$\lim_{T \rightarrow +\infty} \sqrt{T} \lambda(T) = 0, \quad \epsilon(T) = \mathcal{O}(T^{-\alpha}), \quad \text{as } T \rightarrow +\infty, \quad (86)$$

for some $\alpha > 0$.

3. (76) holds for the minimizer $\boldsymbol{\omega}^{(T, \epsilon, \lambda)}$.

Then, as $T \rightarrow +\infty$, $\sqrt{T}(\boldsymbol{\omega}^{(T, \epsilon, \lambda)} - \boldsymbol{\omega}^*)$ converges in distribution to a Gaussian random variable with zero mean and variance matrix \mathcal{F}^{-1} .

Proof. First of all, the condition (86) implies $\lim_{T \rightarrow +\infty} \lambda(T) = 0$. Therefore, Proposition 6 assures that the sequence $\boldsymbol{\omega}^{(T, \epsilon, \lambda)}$ converges to $\boldsymbol{\omega}^*$ almost surely.

The same identity (73) still holds for $\mathcal{M}_j^{(T, \epsilon)}$ and $\boldsymbol{\omega}^{(T, \epsilon, \lambda)}$ in the current setting. Similar to the identity (75), using the relation (43), in the current case we can obtain

$$\sqrt{T} \lambda(T) \mathbf{v}^{(T)} + \mathcal{W}^{(T)} = \mathcal{B}^{(T)} \left[\sqrt{T} (\boldsymbol{\omega}^{(T, \epsilon, \lambda)} - \boldsymbol{\omega}^*) \right],$$

where the vector $\mathbf{v}^{(T)} \in -\partial|\boldsymbol{\omega}|(\boldsymbol{\omega}^{(T, \epsilon, \lambda)})$ is bounded, and $\mathcal{W}^{(T)} \in \mathbb{R}^N$, $\mathcal{B}^{(T)} \in \mathbb{R}^{N \times N}$ are given by

$$\begin{aligned} \mathcal{W}_j^{(T)} &= \frac{1}{\sqrt{T}} \int_0^T (\ln G_\epsilon)' \left(\sum_{j' \in \mathcal{I}_i} \omega_{j'}^* \varphi_{j'}(X(s)) \right) \varphi_j(X(s)) d\tilde{R}_i(s) \\ &\quad - \frac{1}{\sqrt{T}} \int_0^T G'_\epsilon \left(\sum_{j' \in \mathcal{I}_i} \omega_{j'}^* \varphi_{j'}(X(s)) \right) \varphi_j(X(s)) \left[1 - \left(\frac{G_0}{G_\epsilon} \right) \left(\sum_{j' \in \mathcal{I}_i} \omega_{j'}^* \varphi_{j'}(X(s)) \right) \right] ds, \\ \mathcal{B}_{j, j'}^{(T)} &= -\frac{1}{T} \int_0^T \left[\int_0^1 (\ln G_\epsilon)'' \left(\sum_{k \in \mathcal{I}_i} (\theta \omega_k^{(T, \epsilon, \lambda)} + (1 - \theta) \omega_k^*) \varphi_k(X(s)) \right) d\theta \right] \varphi_j(X(s)) \varphi_{j'}(X(s)) dR_i(s) \\ &\quad + \frac{1}{T} \int_0^T \left[\int_0^1 G''_\epsilon \left(\sum_{k \in \mathcal{I}_i} (\theta \omega_k^{(T, \epsilon, \lambda)} + (1 - \theta) \omega_k^*) \varphi_k(X(s)) \right) d\theta \right] \varphi_j(X(s)) \varphi_{j'}(X(s)) ds \end{aligned} \quad (87)$$

if there is an index i , $1 \leq i \leq K$, such that $j, j' \in \mathcal{I}_i$, and otherwise $\mathcal{B}_{j, j'}^{(T)} = 0$.

From Lemma 4 in Appendix A, we have

$$G'_\epsilon(x) \left(1 - \frac{G_0(x)}{G_\epsilon(x)} \right) < \begin{cases} \frac{\epsilon e^{-c/\epsilon}}{c}, & x \geq c, \\ e^{-c/\epsilon}, & x \leq -c, \end{cases} \quad \text{and} \quad G''_\epsilon(x) \leq \frac{1}{\epsilon} e^{-c/\epsilon}, \quad \forall |x| \geq c.$$

Since $\epsilon = \mathcal{O}(T^{-\alpha})$ and the functions φ_j are bounded, we know that the second terms in the expressions of both $\mathcal{W}_j^{(T)}$ and $\mathcal{B}_{j, j'}^{(T)}$ in (87) converge to zero as $T \rightarrow +\infty$. Lemma 5 in Appendix A implies that $\lim_{\epsilon \rightarrow 0+} (\ln G_\epsilon)'(x) = \frac{1}{x}$ and $\lim_{\epsilon \rightarrow 0+} (\ln G_\epsilon)''(x) = -\frac{1}{x^2}$, uniformly on $x \geq c > 0$.

Therefore, Lemma 7 in Appendix B implies that the vector $\mathcal{W}^{(T)}$ converges in distribution to a Gaussian random variable whose mean equals zero and whose variance matrix is given by \mathcal{F} . Since $\lim_{T \rightarrow +\infty} \omega^{(T, \epsilon, \lambda)} = \omega^*$, almost surely, Lemma 6 in Appendix B implies

$$\lim_{T \rightarrow \infty} \mathcal{B}^{(T)} = \mathcal{F}, \quad a.s.$$

Applying Slutsky's Theorem [16] and the condition (86), we conclude

$$\sqrt{T}(\omega^{(T, \epsilon, \lambda)} - \omega^*) = (\mathcal{B}^{(T)})^{-1}(\mathcal{W}^{(T)} + \sqrt{T}\lambda(T)\mathbf{v}^{(T)}) \implies \mathcal{Z} \in \mathcal{N}(0, \mathcal{F}^{-1}),$$

when $T \rightarrow \infty$. □

Acknowledgements

The authors acknowledge financial support from the Einstein Center of Mathematics (EC-Math) through project CH21.

References

- [1] D. F. Anderson and T. G. Kurtz. Continuous time Markov chain models for chemical reaction networks. In H. Koepl, G. Setti, M. di Bernardo, and D. Densmore, editors, *Design and Analysis of Biomolecular Circuits: Engineering Approaches to Systems and Synthetic Biology*, pages 3–42. Springer New York, New York, NY, 2011.
- [2] D. Angeli. A tutorial on chemical reaction network dynamics. *Eur. J. Control*, 15(3):398 – 406, 2009.
- [3] M. Ashyraliyev, Y. Fomekong-Nanfack, J. A. Kaandorp, and J. G. Blom. Systems biology: parameter estimation for biochemical models. *FEBS J.*, 276(4):886–902, 2009.
- [4] A. Bagirov, N. Karmitsa, and M. M. Mäkelä. *Introduction to Nonsmooth Optimization: Theory, Practice and Software*. Springer Publishing Company, Incorporated, 2014.
- [5] K. Ball, T. G. Kurtz, L. Popovic, and G. Rempala. Asymptotic analysis of multiscale approximations to reaction networks. *Ann. Appl. Probab.*, 16(4):1925–1961, 2006.
- [6] A.-L. Barabási and Z. N. Oltvai. Network biology: Understanding the cell's functional organization. *Nat. Rev. Genet.*, 5:101–113, 2004.
- [7] A. Beck and M. Teboulle. A fast iterative shrinkage-thresholding algorithm for linear inverse problems. *SIAM J. Imaging Sci.*, 2(1):183–202, 2009.
- [8] L. Boninsegna, F. Nüske, and C. Clementi. Sparse learning of stochastic dynamical equations. *J. Chem. Phys.*, 148(24):241723, 2018.
- [9] R. J. Boys, D. J. Wilkinson, and T. B. L. Kirkwood. Bayesian inference for a discretely observed stochastic kinetic model. *Stat. Comput.*, 18(2):125–135, 2008.

- [10] S. L. Brunton, J. L. Proctor, and J. N. Kutz. Discovering governing equations from data by sparse identification of nonlinear dynamical systems. *Proc. Natl. Acad. Sci. USA*, 113(15):3932–3937, 2016.
- [11] D. Camacho, P. Vera Licona, P. Mendes, and R. Laubenbacher. Comparison of reverse-engineering methods using an in silico network. *Ann. N. Y. Acad. Sci.*, 1115(1):73–89, 2007.
- [12] F. Clarke. *Optimization and Nonsmooth Analysis*. Classics in Applied Mathematics. SIAM, Philadelphia, PA, 1990.
- [13] B. C. Daniels and I. Nemenman. Efficient inference of parsimonious phenomenological models of cellular dynamics using S-systems and alternating regression. *PLOS ONE*, 10(3):1–14, 2015.
- [14] P. Érdi and J. Tóth. *Mathematical Models of Chemical Reactions: Theory and Applications of Deterministic and Stochastic Models*. Nonlinear science : theory and applications. Manchester University Press, 1989.
- [15] S. Ethier and T. Kurtz. *Markov processes: characterization and convergence*. Wiley series in probability and mathematical statistics. Probability and mathematical statistics. Wiley, 1986.
- [16] T. S. Ferguson. *A Course in Large Sample Theory*. Chapman & Hall Texts in Statistical Science Series. Taylor & Francis, 1996.
- [17] D. T. Gillespie. A general method for numerically simulating the stochastic time evolution of coupled chemical reactions. *J. Comput. Phys.*, 22(4):403 – 434, 1976.
- [18] D. T. Gillespie. Exact stochastic simulation of coupled chemical reactions. *J. Phys. Chem.*, 81(25):2340–2361, 1977.
- [19] D. T. Gillespie. Stochastic simulation of chemical kinetics. *Annu. Rev. Phys. Chem.*, 58(1):35–55, 2007.
- [20] J. Gunawardena. Chemical reaction network theory for in-silico biologists contents. <http://vcp.med.harvard.edu/papers/crnt.pdf>, 2003.
- [21] E. L. Haseltine and J. B. Rawlings. Approximate simulation of coupled fast and slow reactions for stochastic chemical kinetics. *J. Chem. Phys.*, 117(15):6959–6969, 2002.
- [22] T. Hastie, R. Tibshirani, and M. Wainwright. *Statistical Learning with Sparsity: The Lasso and Generalizations*. Chapman and Hall/CRC Monographs on Statistics and Applied Probability. 1st edition, 2015.
- [23] S. Hug, A. Raue, J. Hasenauer, J. Bachmann, U. Klingmüller, J. Timmer, and F. J. Theis. High-dimensional Bayesian parameter estimation: Case study for a model of JAK2/STAT5 signaling. *Math. Biosci.*, 246(2):293 – 304, 2013.
- [24] H.-W. Kang and T. G. Kurtz. Separation of time-scales and model reduction for stochastic reaction networks. *Ann. Appl. Probab.*, 23(2):529–583, 2013.

- [25] S. Kar, W. T. Baumann, M. R. Paul, and J. J. Tyson. Exploring the roles of noise in the eukaryotic cell cycle. *Proc. Natl. Acad. Sci. USA*, 106(16):6471–6476, 2009.
- [26] A. Klimovskaia, S. Ganscha, and M. Claassen. Sparse regression based structure learning of stochastic reaction networks from single cell snapshot time series. *PLOS Comput. Biol.*, 12:1–20, 2016.
- [27] J. N. Kutz. *Data-Driven Modeling & Scientific Computation: Methods for Complex Systems & Big Data*. OUP Oxford, 1st edition, 2013.
- [28] E. Lehmann. *Elements of Large-Sample Theory*. Springer Texts in Statistics. Springer New York, 2004.
- [29] D. Machado, R. S. Costa, M. Rocha, E. C. Ferreira, B. Tidor, and I. Rocha. Modeling formalisms in systems biology. *AMB Express*, 1(1):45, 2011.
- [30] D. J. C. MacKay. *Information Theory, Inference, and Learning Algorithms*. Cambridge University Press, New York, NY, USA, 2002.
- [31] N. M. Mangan, S. L. Brunton, J. L. Proctor, and J. N. Kutz. Inferring biological networks by sparse identification of nonlinear dynamics. *IEEE Trans. Mol. Biol. Multi-Scale Commun.*, 2(1):52–63, 2016.
- [32] S. P. Meyn and R. L. Tweedie. *Markov Chains and Stochastic Stability*. Springer-Verlag, London, 1993.
- [33] C. A. Penfold and D. L. Wild. How to infer gene networks from expression profiles, revisited. *Interface Focus*, 1(6):857–870, 2011.
- [34] S. Reinker, R. M. Altman, and J. Timmer. Parameter estimation in stochastic biochemical reactions. *IEE P. Syst. Biol.*, 153(4):168–178, 2006.
- [35] R. Srivastava, L. You, J. Summers, and J. Yin. Stochastic vs. deterministic modeling of intracellular viral kinetics. *J. Theor. Biol.*, 218(3):309–321, 2002.
- [36] P. S. Swain, M. B. Elowitz, and E. D. Siggia. Intrinsic and extrinsic contributions to stochasticity in gene expression. *Proc. Natl. Acad. Sci. USA*, 99(20):12795–12800, 2002.
- [37] N. Tenazinha and S. Vinga. A survey on methods for modeling and analyzing integrated biological networks. *IEEE/ACM Trans. Comput. Biol. Bioinform.*, 8(4):943–958, 2011.
- [38] R. Tibshirani. Regression shrinkage and selection via the Lasso. *J. R. Statist. Soc. B (Methodological)*, 58(1):267–288, 1996.
- [39] R. Tibshirani. Regression shrinkage and selection via the lasso: a retrospective. *J. R. Statist. Soc. B (Statistical Methodology)*, 73(3):273–282, 2011.
- [40] G. Tran and R. Ward. Exact recovery of chaotic systems from highly corrupted data. *Multiscale Model. & Simul.*, 15(3):1108–1129, 2017.
- [41] A. F. Villaverde and J. R. Banga. Reverse engineering and identification in systems biology: strategies, perspectives and challenges. *J. R. Soc. Interface*, 11(91), 2014.

- [42] W.-X. Wang, R. Yang, Y.-C. Lai, V. Kovanis, and C. Grebogi. Predicting catastrophes in nonlinear dynamical systems by compressive sensing. *Phys. Rev. Lett.*, 106:154101, 2011.
- [43] D. J. Wilkinson. *Stochastic Modelling for Systems Biology, Second Edition*. Chapman & Hall/CRC Mathematical and Computational Biology. Taylor & Francis, 2011.

A Properties of the function G_ϵ

In this section, we summarize some asymptotic properties of the function G_ϵ in (32). Given $\epsilon > 0$, recall that

$$G_\epsilon(x) = \epsilon \ln(1 + e^{x/\epsilon}), \quad \forall x \in \mathbb{R},$$

whose first and second derivatives are

$$G'_\epsilon(x) = \frac{e^{x/\epsilon}}{1 + e^{x/\epsilon}}, \quad G''_\epsilon(x) = \frac{1}{\epsilon} \frac{e^{x/\epsilon}}{(1 + e^{x/\epsilon})^2}, \quad (88)$$

respectively. The following lemma can be easily proved and therefore its proof is omitted.

Lemma 4. *Given $\epsilon > 0$, we have the following estimates.*

1. $\max(x, 0) < G_\epsilon(x) \leq \max(x, 0) + \epsilon \ln 2, \quad \forall x \in \mathbb{R}.$
2. $1 - e^{-x/\epsilon} < G'_\epsilon(x) < 1$, if $x \geq 0$, and $0 < G'_\epsilon(x) < e^{x/\epsilon}$, if $x < 0$.
3. $0 < G''_\epsilon(x) < \frac{1}{\epsilon} e^{-|x|/\epsilon}, \quad \forall x \in \mathbb{R}.$

In particular, Lemma 4 implies that

$$\lim_{\epsilon \rightarrow 0+} G_\epsilon(x) = \max(x, 0),$$

uniformly for $x \in \mathbb{R}$, and we have

$$\lim_{\epsilon \rightarrow 0+} G'_\epsilon(x) = \begin{cases} 1, & x > 0, \\ \frac{1}{2}, & x = 0, \\ 0, & x < 0, \end{cases} \quad \lim_{\epsilon \rightarrow 0+} G''_\epsilon(x) = \begin{cases} 0, & x \neq 0, \\ +\infty, & x = 0. \end{cases}$$

In this work, we also need the function

$$\ln G_\epsilon(x) = \ln [\epsilon \ln(1 + e^{x/\epsilon})],$$

whose first and second derivatives are

$$\begin{aligned} (\ln G_\epsilon)'(x) &= \frac{e^{x/\epsilon}}{\epsilon(1 + e^{x/\epsilon}) \ln(1 + e^{x/\epsilon})}, \\ (\ln G_\epsilon)''(x) &= \frac{1}{\epsilon^2} \frac{e^{x/\epsilon}}{(1 + e^{x/\epsilon})^2} \frac{1}{\ln(1 + e^{x/\epsilon})} \left[1 - \frac{e^{x/\epsilon}}{\ln(1 + e^{x/\epsilon})} \right]. \end{aligned} \quad (89)$$

Lemma 5. *Given $\epsilon > 0$, we have the following estimates.*

1. $\forall x > 0$, we have

$$\begin{aligned} \ln x &< \ln G_\epsilon(x) < \ln x + \frac{\epsilon}{x} e^{-x/\epsilon}, \\ \frac{1}{(1 + e^{-x/\epsilon})(x + \epsilon \ln 2)} &< (\ln G_\epsilon)'(x) < \frac{1}{x}, \\ -\frac{1}{x^2} &< (\ln G_\epsilon)''(x) < \frac{e^{-x/\epsilon}}{\epsilon x} - \frac{1}{(1 + e^{-x/\epsilon})^2 (x + \epsilon \ln 2)^2}. \end{aligned} \quad (90)$$

2. For $x = 0$, we have

$$\begin{aligned} \ln G_\epsilon(0) &= \ln \epsilon + \ln \ln 2, \quad (\ln G_\epsilon)'(0) = \frac{1}{(2 \ln 2) \epsilon}, \\ (\ln G_\epsilon)''(0) &= \frac{1}{4 \ln 2} \left(1 - \frac{1}{\ln 2}\right) \frac{1}{\epsilon^2}. \end{aligned}$$

3. $\forall x < 0$, we have

$$\begin{aligned} \ln G_\epsilon(x) &< \ln \epsilon + \frac{x}{\epsilon}, \quad (\ln G_\epsilon)'(x) > \frac{1}{2\epsilon}, \\ -\frac{2}{\epsilon^2} e^{x/\epsilon} &< (\ln G_\epsilon)''(x) < 0. \end{aligned}$$

Proof. We will only prove the inequalities concerning $(\ln G_\epsilon)''$.

1. When $x > 0$, using (89) and the fact $\epsilon \ln(1 + e^{x/\epsilon}) > x$, we have

$$(\ln G_\epsilon)''(x) > -\frac{1}{x^2}.$$

For the upper bound, using Lemma 4, we have

$$\begin{aligned} \frac{1}{\epsilon^2} \frac{e^{x/\epsilon}}{(1 + e^{x/\epsilon})^2} \frac{1}{\ln(1 + e^{x/\epsilon})} &= \frac{1}{\epsilon^2} \frac{e^{-x/\epsilon}}{(1 + e^{-x/\epsilon})^2} \frac{1}{\ln(1 + e^{x/\epsilon})} < \frac{e^{-x/\epsilon}}{\epsilon x}, \\ -\frac{e^{2x/\epsilon}}{(1 + e^{x/\epsilon})^2} \frac{1}{[\epsilon \ln(1 + e^{x/\epsilon})]^2} &\leq -\frac{1}{(1 + e^{-x/\epsilon})^2} \frac{1}{(x + \epsilon \ln 2)^2}, \end{aligned}$$

and therefore (90) is obtained.

2. When $x < 0$, using the fact that $-\frac{u^2}{2} < \ln(1 + u) - u < 0$, for $\forall u > 0$, we have

$$\ln(1 + e^{x/\epsilon}) > e^{x/\epsilon} - \frac{1}{2} e^{2x/\epsilon} > \frac{1}{2} e^{x/\epsilon}.$$

Therefore,

$$\begin{aligned} (\ln G_\epsilon)''(x) &= \frac{e^{x/\epsilon}}{\epsilon^2 (1 + e^{x/\epsilon})^2} \frac{1}{(\ln(1 + e^{x/\epsilon}))^2} (\ln(1 + e^{x/\epsilon}) - e^{x/\epsilon}) \\ &> -\frac{e^{3x/\epsilon}}{2\epsilon^2 (1 + e^{x/\epsilon})^2} \frac{1}{\frac{1}{4} e^{2x/\epsilon}} > -\frac{2}{\epsilon^2} e^{x/\epsilon}. \end{aligned} \quad \square$$

Summarizing the estimates in Lemma 5, we can conclude that

$$\lim_{\epsilon \rightarrow 0+} \ln G_\epsilon(x) = \begin{cases} \ln x, & x > 0, \\ -\infty, & x \leq 0, \end{cases} \quad \lim_{\epsilon \rightarrow 0+} (\ln G_\epsilon)'(x) = \begin{cases} \frac{1}{x}, & x > 0, \\ +\infty, & x \leq 0, \end{cases}$$

$$\text{and } \lim_{\epsilon \rightarrow 0+} (\ln G_\epsilon)''(x) = \begin{cases} -\frac{1}{x^2}, & x > 0, \\ -\infty, & x = 0, \\ 0, & x < 0. \end{cases}$$

B Two limit lemmas on integrations with respect to counting processes

In this section, we summarize two useful results concerning integrations with respect to the processes R_i, \tilde{R}_i in (56) and (57), respectively. These results play an important role in the asymptotic analysis in Section 5.

The first result is a type of law of large numbers (LLN) for Poisson processes.

Lemma 6. *Suppose that Assumption 1 holds. Functions $f^{(T)} : \mathbb{X} \rightarrow \mathbb{R}$ are uniformly bounded such that $\lim_{T \rightarrow +\infty} f^{(T)} = f$, uniformly on \mathbb{X} . For each $1 \leq i \leq K$, we have*

$$\lim_{T \rightarrow +\infty} \frac{1}{T} \int_0^T f^{(T)}(X(s)) dR_i(s) = \sum_{x \in \mathbb{X}} f(x) a_i^*(x) \pi(x), \quad a.s. \quad (91)$$

and

$$\lim_{T \rightarrow +\infty} \frac{1}{T} \int_0^T f^{(T)}(X(s)) d\tilde{R}_i(s) = 0, \quad a.s. \quad (92)$$

Proof. Using the LLN of Poisson processes in (63) and the uniform convergence of $f^{(T)}$, we have

$$\begin{aligned} & \left| \lim_{T \rightarrow +\infty} \frac{1}{T} \int_0^T f^{(T)}(X(s)) dR_i(s) - \lim_{T \rightarrow +\infty} \frac{1}{T} \int_0^T f(X(s)) dR_i(s) \right| \\ & \leq \lim_{T \rightarrow +\infty} \left[\frac{R_i(T)}{T} \sup_{x \in \mathbb{X}} |f^{(T)} - f| \right] = 0. \end{aligned}$$

Therefore, it is sufficient to prove (91) for the case $f^{(T)} \equiv f$. Note that we have

$$\frac{1}{T} \int_0^T f(X(s)) dR_i(s) = \sum_{x \in \mathbb{X}} \left[f(x) \frac{1}{T} \int_0^T \mathbf{1}_x(X(s)) dR_i(s) \right], \quad (93)$$

where $\mathbf{1}_x$ denotes the indicator function at state x . For each $x \in \mathbb{X}$, the integration

$$\int_0^T \mathbf{1}_x(X(s)) dR_i(s)$$

can be interpreted as the total number that the i th channel \mathcal{C}_i becomes active within time $[0, T]$ when the state of the system is x . Similarly, $\int_0^T \mathbf{1}_x(X(s)) ds$ can be interpreted as the total time that the system spends at state x within time $[0, T]$. Since the waiting times at state x before the channel \mathcal{C}_i becomes activated are independent and follow exponential distributions with mean value $(a_i^*(x))^{-1}$, the LLN of exponential distributions implies that

$$\lim_{T \rightarrow +\infty} \frac{\int_0^T \mathbf{1}_x(X(s)) ds}{\int_0^T \mathbf{1}_x(X(s)) dR_i(s)} = \frac{1}{a_i^*(x)}, \quad a.s. \quad (94)$$

Since the system is ergodic (Assumption 1), Birkhoff's ergodic theorem implies

$$\lim_{T \rightarrow +\infty} \frac{1}{T} \int_0^T \mathbf{1}_x(X(s)) ds = \pi(x), \quad a.s. \quad (95)$$

Combining (93)–(95), we obtain

$$\lim_{T \rightarrow +\infty} \frac{1}{T} \int_0^T f(X(s)) dR_i(s) = \sum_{x \in \mathbb{X}} f(x) a_i^*(x) \pi(x), \quad a.s.$$

The conclusion (92) follows as a consequence, using the definition of \tilde{R}_i in (57) and the ergodicity of the system. \square

The second result is a corollary of the martingale central limit theorem [15, Theorem 7.1.4].

Lemma 7. *Suppose that Assumption 1 holds. For each $1 \leq j \leq N$, functions $f_j, f_j^{(T)} : \mathbb{X} \rightarrow \mathbb{R}$ are uniformly bounded such that $\lim_{T \rightarrow +\infty} f_j^{(T)} = f_j$, uniformly on \mathbb{X} . Let $\mathcal{W}^{(T)}(u) \in \mathbb{R}^N$ denote the N -dimensional process whose components are*

$$\mathcal{W}_j^{(T)}(u) = \frac{1}{\sqrt{T}} \int_0^{Tu} f_j^{(T)}(X(s)) d\tilde{R}_i(s), \quad u \geq 0,$$

where $1 \leq j \leq N$, and the index i satisfies $j \in \mathcal{I}_i$. \mathcal{F} is the $N \times N$ matrix with entries given by

$$\mathcal{F}_{j,j'} = \begin{cases} \sum_{x \in \mathbb{X}} f_j(x) f_{j'}(x) a_i^*(x) \pi(x), & \text{if } j, j' \in \mathcal{I}_i, \text{ for some index } 1 \leq i \leq K, \\ 0, & \text{otherwise} \end{cases} \quad (96)$$

for $1 \leq j, j' \leq N$. We define the matrix-valued (linear) process $\mathcal{A}(u) = u\mathcal{F}$, $u \geq 0$.

As $T \rightarrow \infty$, $\mathcal{W}^{(T)}$ converges in distribution to \mathcal{W} , where \mathcal{W} is an N -dimensional process with independent Gaussian increments whose quadratic variation process is \mathcal{A} . In particular, $\mathcal{W}^{(T)}(1)$ converges in distribution to a Gaussian random variable whose mean is zero and whose variance matrix is \mathcal{F} in (96).

Proof. For each $T > 0$, we define the matrix-valued process $\mathcal{A}^{(T)}(u)$, $u \geq 0$, whose components are given by

$$\mathcal{A}_{j,j'}^{(T)}(u) = \begin{cases} \frac{1}{T} \int_0^{Tu} f_j^{(T)}(X(s)) f_{j'}^{(T)}(X(s)) a_i^*(X(s)) ds, & \text{if } j, j' \in \mathcal{I}_i, \text{ for some } 1 \leq i \leq K, \\ 0, & \text{otherwise,} \end{cases} \quad (97)$$

for $1 \leq j, j' \leq N$. Let us verify the conditions required in the martingale central limit theorem [15, Theorem 7.1.4].

Firstly, from (56) and (57), using Ito's formula, we know that the process

$$\mathcal{W}_j^{(T)}(u) \mathcal{W}_{j'}^{(T)}(u) - \mathcal{A}_{j,j'}^{(T)}(u), \quad u \geq 0,$$

is a martingale. Using the expression (97) and the ergodicity of the system, we have

$$\lim_{T \rightarrow +\infty} \mathcal{A}_{j,j'}^{(T)}(u) = u \mathcal{F}_{j,j'} = \mathcal{A}_{j,j'}(u), \quad a.s.$$

Furthermore, for any $u_0 \geq 0$, since the functions $f_j^{(T)}$ are uniformly bounded, we have

$$\lim_{T \rightarrow +\infty} \mathbf{E} \left[\sup_{u \leq u_0} \left| \mathcal{W}_j^{(T)}(u) - \mathcal{W}_j^{(T)}(u-) \right|^2 \right] \leq \lim_{T \rightarrow +\infty} \frac{1}{T} \mathbf{E} \left[\sup_{u \leq Tu_0} \left| f_j^{(T)}(X(u)) \right|^2 \right] = 0.$$

Secondly, because the processes $\mathcal{A}_{j,j'}^{(T)}(u)$ in (97) have continuous paths, the limit

$$\lim_{T \rightarrow +\infty} \mathbf{E} \left[\sup_{u \leq u_0} \left| \mathcal{A}_{j,j'}^{(T)}(u) - \mathcal{A}_{j,j'}^{(T)}(u-) \right| \right] = 0$$

holds trivially, for $1 \leq j, j' \leq N$. Therefore, the conclusion follows from the martingale central limit theorem [15, Theorem 7.1.4]. \square